Development of Cell-laden Hydrogels with High Mechanical Strength for Tissue Engineering Applications

by

Hyeongho Shin

B.S. Chemical Engineering
Seoul National University, 2004

Submitted to the Department of Materials Science and Engineering in partial fulfillment of the requirements for the degree of

Doctor of Philosophy
at the
Massachusetts Institute of Technology

February 2014

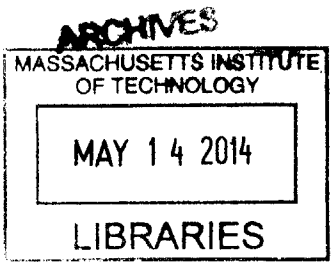

Signature of Author .....
Department of Materials Science and Engineering
October 7, 2013

Certified by .....
Ali Khademhosseini
Associate Professor of Medicine and Health Sciences and Technolgy, Harvard Medical School
Thesis Supervisor

Certified by .....
Christine Ortiz
Professor of Materials Science and Technology
Thesis Reader

Accepted by .....
Gerbrand Ceder
Professor of Materials Science and Engineering
Chair of the Departmental Committee on Graduate Students

Development of Cell-laden Hydrogels with High Mechanical Strength for Tissue Engineering Applications

by

Hyeongho Shin

Submitted to the Department of Materials Science and Engineering
on October 7, 2013 in partial fulfillment of the requirements
for the degree of Doctor of Philosophy in Materials Science and Engineering

Abstract

The development of materials with biomimetic mechanical and biological properties is of great interest for regenerative medicine applications. Hydrogels are a promising class of biomaterials due to several advantages, however, the mechanical weakness remains a critical challenge for applications as tissue scaffolds. Particularly, scaffolds for load-bearing tissues such as cartilage and bone need to have great strength to keep their integrity after implantation. This thesis focused on the development of cell-laden hydrogels that have high mechanical strength and good biological properties. The first work of the thesis was to synthesize a biodegradable hydrogel, poly(glucose malate)methacrylate (PGMma), from two natural monomers glucose and malic acid. The PGMma hydrogels were cell-adhesive, and mechanically tunable by altering the formulation. In the second work, double-network (DN) hydrogels were prepared from two biomacromolecules, gellan gum and gelatin. The DN hydrogels prepared exhibited much higher strength than traditional hydrogels, the maximal strength being 6.9MPa. By using a cell-compatible two-step photocrosslinking process, it was also possible to encapsulate cells with high viability. Further research into the materials as tissue scaffolds showed that the DN hydrogels weakened when they were prepared at cell-compatible conditions, and stronger cell-hydrogel interaction is needed to improve the function of the encapsulated cells. Therefore in the last work, microgel-reinforced (MR) hydrogels that have better mechanical strength and biological properties in comparison to DN hydrogels were prepared by embedding stiff GG microgels into soft and ductile gelatin hydrogels. The MR hydrogels exhibited higher strength than the DN hydrogels and the gelatin hydrogels. The cells encapsulated in MR hydrogels showed high metabolic activity and high level of osteogenic behaviors similar to the cells encapsulated in gelatin hydrogels, which was not the case for DN hydrogels. The MR hydrogels, the final product of all these works could be potentially useful for load-bearing tissue scaffolds.

Thesis Supervisor: Ali Khademhosseini
Title: Associate professor of Medicine and Health Sciences and Technology, Harvard Medical School

Acknowledgements

I would like to thank my advisor Dr. Ali Khademhosseini for his guidance and support throughout my graduate experience at MIT. He provided me with opportunities to learn from many people with various expertises and trained me to be a self-driven and independent scientist that can survive the fast-growing research field.

I thank Dr. Bradley D. Olsen for his guidance and scientific advice on my projects. He understood and encouraged me when I was depressed by the research data. I also thank Dr. Christine Ortiz and Dr. Michael Cima for serving on my thesis committee and for their helpful advices and suggestions.

Dr. Halil Tekin, who had been in the lab for five years with me before he graduated, helped me a lot and was the good friend that I can talk with about the graduate life. Mark Brigham introduced the lab and taught the basics of experiments to me when I joined the lab. Dr. Jason W. Nichol guided my first project and answered my basic questions, which helped me to start my own project.

So many people passed by the lab. Some of them helped me a lot with experiments and gave me good advice on science and the graduate life. Some of them were very nice to encourage me and wish my successful graduation. I thank Dr. Shilpa Sant, Dr. Akhilesh Gaharwar, Dr. Alpesh Petal, Dr. Jesper Hjortnaes, Dr. Neslihan Alemdar, Silvia Mihaila, and many other people. I am sorry to many people that passed by the lab that I could not care, help, and be kind to more because I was too busy and stressed especially for the last two years of my graduate life.

I would like to thank many Korean post-docs who passed by the lab for their kind encouragement and consolation. I have lots of good memories of having good times with them.

PPST friends of my year, Dr. Jane Wang, Yin Fan, Adam Zeiger, and Alex W. Scott have been my good friends. They kept me from feeling lonely and helped me to adjust to the foreign academic life. I hope all of them can continue their successful career somewhere in the world.

Korean PPST friends, Dr. Seungwoo Lee and Hyewon Kim helped me a lot in preparing the qualifying exam, and encouraged me throughout the graduate experience. KGMSE friends of my year, Hyunjeong Lee, Jaechul Kim, Heechul Park, and Shinyoung Kang, have been my closest friends. Thanks to them, I have lots of good memories of my MIT life.

People from my church, FKCC, prayed for me and encouraged me. Dr. Soochan Bae, Dr. Jonghwan Kim, Dr. Changhyun Sung were my great mentors. Thanks to many friends from the church, my life in the USA has been more pleasant.

I could not be here without the support, prayer, and love of my mom and dad. I love you. And my sister, she is always supporting me in her heart.

To my wife, Eunkyoung Lee, who has been my greatest support and I will share all my happy life with, thank you, and I love you.

Table of contents

List of figures

List of tables

Chapter 1: Introduction and background

1.1. Scaffolds for tissue engineering

The general strategy to create new organs or tissues is to seed appropriate cells into biodegradable scaffold, and culture them with various environmental factors in order for the cells to make their own extracellular matrix (ECM) and form a new tissue structure, while the scaffold degrades away [1]. Scientists have been studying about the three major components of tissue engineering, which are cells, environmental factors, and scaffolds. First, an adequate source of healthy, expandable cells is required to obtain a large amount of cells enough to engineer tissue constructs, thus autologous, allogeneic, and xenogeneic cells are being studied respectively for engineered implants [2]. Stem cells are a promising candidate for treating tissues where the source of cells is limited [3], and methods to better handle them are actively being examined. Second, various environmental factors such as growth factors, mechanical forces, and ECM molecules affect growth and function of cells. They selectively interact with specific stimulus receptors expressed on the surface of cells to facilitate repairs of damaged tissues [4].

The scaffold is also a very important part of tissue engineering as it accommodates cells and guides their growth in three dimensional tissues. There are several requirements in the design of scaffolds. They have to be biocompatible, biodegradable, porous and permeable, exhibit adequate mechanical properties, and possess surface chemistry for cell attachment [5]. Metals and ceramics have been used extensively for surgical implantations, but most of them are not biodegradable, and their proscessability is very limited [6]. Due to these reasons, polymers have become a promising candidate for scaffolds. Natural polymers such as collagen and chitosan closely mimic the native cellular environment, so they have been studied widely to repair various tissues. Biodegradable synthetic polymers such as poly(α-hydroxy ester)s, poly(ortho esters), and polyanhydrides were developed as alternatives to natural polymers [7]. Synthetic polymers can be prepared with controllable and reproducible properties, and most of them degrade by chemical hydrolysis, not by enzymatic processes, so their degradation does not depend on the patient. However, many of them produce acidic degradation products which

can harm cells, and they are hydrophobic and typically prepared in severe conditions preventing from encapsulating viable cells to provide three-dimensional environment [8].

1.2. Hydrogels as tissue scaffolds

Hydrogels are a network of hydrophilic polymer chains that contain a large amount of water. Hydrogels have received great attention as tissue scaffolds due to their high water content, biocompatibility, and good permeability for transport of nutrients and wastes. It can also be injected into the body in a minimally invasive method, and encapsulate cells to provide three-dimensional environment which mimics native tissues more closely [8, 9]. Various synthetic and natural materials can be used to form hydrogels as tissue scaffolds. Synthetic materials include poly(ethylene glycol), poly(vinyl alcohol), poly(acrylic acid), and polypeptides. Natural materials include proteins and polysaccharides such as collagen, gelatin, chitosan, alginate, and hyaluronic acid. Hydrogels can be formed by inherent phase transition, ionic crosslinking, or covalent crosslinking. For example, collagen forms hydrogel by temperature-driven phase transition, but it is too soft to handle [10]. Alginate forms hydrogel by ionic crosslinking with multivalent cations, however, ionic crosslinking is not stable due to exchange of ions with other ionic molecules in aqueous solutions [11]. Covalent crosslinking is more stable, resulting in relatively stiff hydrogel, but most of the chemical crosslinkers are toxic to cells. Thus, a covalent crosslinking method that is cell-compatible may be desirable.

1.2.1. Photocrosslinked hydrogels

As a way of cell-compatible crosslinking, photocrosslinking has been widely used for tissue scaffold studies. Polymers are modified to become photocrosslinkable by functionalizing with photoreactive moieties such as acrylate or methacrylate groups before they are dissolved with photoinitiator and exposed to light. Then the initiator creates radicals that are transferred to the photoreactive groups to undergo chain polymerization. Studies have shown that by using mild conditions (light intensity, kind and the amount of photoinitiator, and exposure time), photocrosslinking is compatible with encapsulation of a variety of cells [12, 13]. Besides cell-

compatibility, this method enables temporal and spatial control in the fabrication of complicated structures [14, 15]. For example, control of light by using masks can make asymmetrical matrix environment, which leads to spatially patterned differentiation of embryonic stem cells [16]. The photoreactive groups can be attached to any polymers with pendant functional groups such as hydroxyl or amine groups, and the process is very simple. Most of the common natural polymers such as collagen [17, 18], gelatin [19-21], chitosan [22, 23], alginate [24, 25], dextran [26-28], and hyaluronic acid [29-31] have been modified to form photocrosslinked hydrogels for tissue engineering researches. Given these advantages, photocrosslinked hydrogels are a powerful tool in developing tissue constructs.

1.3. Hydrogels with high mechanical strength

The mechanical properties of native tissues vary depending on their functions. The softest tissues such as brain and liver exhibit the modulus of hundreds of Pa, while lung and cardiac muscle are stiffer with the modulus ranging from several to a few hundred kPas [32]. Load-bearing tissues such as cartilage, tendon, and bone exhibit much higher modulus, which is on the order of MPa or even up to GPa [32, 33]. These load-bearing tissues have strength of a few tens to a few hundred MPas, which is enough to prevent from failure of the tissues by frequent loads [34-36]. It has been a main challenge to create tissue scaffolds of which the mechanical properties closely mimic the native tissues. In particular, despite several advantages of hydrogels as tissue scaffolds, the mechanical weakness of hydrogels is a critical defect in using them as load-bearing tissue scaffolds. The strength of most traditional hydrogels is below 1 MPa [37-40]. Thus, several new platform materials have been developed to improve the mechanical strength of hydrogels.

A main reason that traditionally crosslinked hydrogels are weak is the heterogeneous distribution of crosslinks that result in concentrated stress around the dense crosslinks [41]. Thus, some studies used an approach of making homogenous crosslinks distribution for uniform distribution of stress. Tetra-PEG hydrogel [42] was designed by combining two tetrahedron-like PEG macromers of the same size. By terminating the four arms of each macromer with

functional groups that can react with each other, the two macromers were connected alternately so the resulting hydrogel had a homogeneous network structure leading to high mechanical strength. Polyrotaxane hydrogel [43] consisted of poly(ethylene glycol) (PEG) chains and α-cyclodextrin molecules threaded and trapped by large end groups on the PEG chains. These α-cyclodextrin molecules were chemically crosslinked, so the crosslinkers could slide to distribute the tension evenly throughout the hydrogel, resulting in highly stretchable hydrogel. Nanocomposite hydrogel [44] was prepared by mixing clay slabs and *N*-isopropyl acrylamide (NIPAM) monomers followed by radical polymerization of the NIPAM monomers. The clay slabs served as multifunctional crosslinkers dispersed uniformly to distribute tension and make the polymer chains connected to the same clays withstand the load cooperatively.

Self-assembly of copolymers was also used to develop strong hydrogels. Ionically crosslinked triblock copolymer hydrogel [45] was prepared by synthesizing an amphiphilic triblock copolymer consisting of two glassy poly(methyl methacrylate) end blocks and a poly(methacrylic acid) midblock. The ionic crosslinking among carboxylate groups in conjunction with the self-assembled triblock copolymer network resulted in high mechanical strength. A responsive block copolymer composed of poly(N-isopropylacrylamide) (PNIPAM) end blocks and a protein midblock containing coiled-coil associating domains was also developed [46]. The thermoresponsive self-assembly of PNIPAM blocks reinforced the shear thinning hydrogel formed by the association of the engineered protein blocks.

Although strong hydrogels have been prepared using various strategies as explained above, challenges exist in using them as tissue engineering scaffolds, such as cytotoxic, non-biodegradable materials, cytotoxic processing conditions, and insufficient strength. Modifications to these approaches are needed to make the hydrogels biodegradable and enable cell-compatible processing conditions and better cell-hydrogel interaction.

1.3.1. Double-network (DN) and microgel-reinforced (MR) hydrogels

Another approach to make a strong hydrogel is through the use of double-network (DN) molecular approach. DN hydrogel consists of two networks with opposing mechanical

properties, one being stiff and brittle and the other being soft and ductile. Combination of these two networks with different mechanical properties results in the formation of strong hydrogels. Several DN hydrogels have been prepared from various materials. Gong et al. used highly crosslinked poly(2-acrylamido-2-methylpropanesulfonic acid) (PAMPS) and loosely crosslinked poly(acrylamide) (PAAm) [47]. *N,N'*-methylenebisacrylamide (MBAA), a chemical crosslinker, was used to control the crosslink density of each network. Waters et al. prepared DN hydrogels by photocrosslinking PEG and poly(acrylic acid) sequentially [48]. Natural polymers were also used to create DN hydrogels. Nakayama et al. created bacterial cellulose-based hydrogels which exhibit anisotropic mechanical properties by adding gelatin or polysaccharides such as gellan gum, alginate, and carrageenan physically crosslinked [49]. Weng et al. used methacrylated hyaluronic acid and N,N-dimethylacrylamide to prepare strong hydrogels for corneal implant applications [50].

Gong et al. studied extensively on the structure and strengthening mechanism of their DN hydrogels. With the data obtained by using dynamic light scattering, they proposed a structure model in which the PAMPS network is inhomogeneous and voids exist due to the radical polymerization [51]. The PAAm network interpenetrates in the PAMPS network and also fills the voids, absorbing the energy needed for crack propagation in the PAMPS network. It was also found that a large damage zone is formed around a crack tip which prevents the crack propagation, and the rigid network fragments into small clusters, which plays a role of crosslinkers correcting the inequality of stress [41, 52]. The effects of several parameters on the strength of DN hydrogel were also studied. The significant enhancement of strength of DN hydrogels was obtained only when the molar ratio of the second to the first polymer was as high as several to a few tens. In addition, an optimal crosslink density for the second network existed, that with higher crosslink density lowering the strength [47]. The molecular weight of the second polymer was also an important parameter for strengthening the DN hydrogels, with a critical value for a remarkable enhancement [53]. High concentration of the second polymer was needed for more entanglement with each other [53, 54]. It was also found that the addition of a small amount of voids into the first network increased the strength of the DN hydrogels. The

voids led to concentrated stress around them which allowed wider range of internal fracture of the first network [55].

Knowing that strengthening of the DN hydrogels is due to the first network that helps to dissipate the stress, Gong et al. also tried to introduce PAMPS microgels into PAAm hydrogels as a strengthening motif of the same manner [56, 57]. The microgel-reinforced (MR) hydrogels exhibited significant enhancement in mechanical strength in comparison to the hydrogels with no mirogels, and they showed comparable mechanical properties with the DN hydrogels prepared from the same polymers. It was found that the two parameters, the concentration of the microgels in the MR hydrogels and the molar ratio of the two polymers in the microgel phase were critical in the strength of the MR hydrogels.

Similar approaches that used microgels to reinforce hydrogels have also been developed. For example, Qin et al. prepared hydrogels containing hydrophilic reactive microgels (HRM) by embedding PAAm microgels into PAAm/PAMPS hydrogels [58]. The PAAm microgels were modified with C=C double bond so that they could be covalently linked to the PAAm/PAMPS hydrogels. By altering the microgel concentration in the HRM hydrogels and the mass ratio of PAAm/PAMPS, the strength of hydrogels were tuned. Lally et al. added either ethyleneglycol dimethacrylate or PEG dimethacrylate as a crosslinking monomers in a dispersion of pH-responsive poly (ethylacrylate/methacrylic acid/butanediol diacrylate) microgels and crosslinked the monomers [59]. The mechanical properties of the resulting hydrogels were tunable by changing the pH or the type of the crosslinking monomers. Jha et al. prepared hyaluronic acid microgels modified with methacrylate groups [60]. The microgels were then integrated by covalent bonds in the bulk hydrogel from methacrylated hyaluronic acid resulting in stronger hydrogels. Chondrocytes could be encapsulated in these hydrogels with minimal cell damage, and they produced cartilage specific extracelluar matrix.

However, these strategies that used DN or microgel approach still have limitations in using them as tissue scaffolds such as non-biodegradable materials, cytotoxic processing conditions, and poor cell-matrix interaction.

1.4. Bone tissue engineering

Bone is a composite material consisting of 65-70% hydroxylapatite mineral part, and 25-30% organic part [61]. It is arranged in two architectural forms, which are trabecular or cancellous bone that composes about 20% of the total skeleton and cortical or compact bone that composes about 80% of the total skeleton [62]. Cortical bone is very stiff and strong, being about 10% porous, while trabecular bone has a high porosity of 50-90% exhibiting around 20 times inferior stiffness and strength than cortical bone [62]. The proportion of these two types of bone differs depending on locations in a body. Bone tissue is maintained by the interaction of three cell types: osteoblasts, which synthesize and regulate bone ECM deposition and mineralization, osteocytes (former osteoblasts entrapped in mineral), which play as a sensor and information transfer system, and osteoclasts, which resorbs bone [63].

Roughly one million cases of bone defects are occurring each year and treating these defects is raising more concern due to the ageing of population [63]. Autologous and allogeneic bone grafting have been effective in alleviating the disability, but they have limitations such as insufficient donor tissue, immune rejection, donor site morbidity, and pathogen transmission [64]. Metals and ceramic were also used as alternatives, but they also presented disadvantages such as poor overall integration with native tissue and mechanical mismatch [63]. Bone tissue engineering thus has been actively investigated to overcome these issues. There are two critical components to engineer bone tissue: cells and scaffolds.

Obtaining a sufficient amount of appropriate cells is essential to engineer tissue construct. The obvious choice of cells for bone tissue engineering is osteoblasts. However, only a small amount can be obtained after isolation of osteoblasts, and their growth rate is relatively low [63]. In addition, in case of autologous cells from a patient with bone related diseases, the protein expression of the osteoblasts may be under the normal values [65]. Stem cells are a great alternative since they can be easily isolated and expanded *in vitro*. The finding that the embryonic stem cells differentiated into osteoblasts in the presence of dexamethasone was of particular interest for bone tissue engineering [66]. Due to ethical concerns with embryonic stem cells, mesenchymal stem cells (MSCs) isolated from bone marrow, which were found to be able to differentiate into osteoblasts in the adequate culture condition [67], are being used broadly in

bone tissue engineering research. The osteogenic differentiation of MSCs is influenced by many factors, but they are usually cultured in media containing L-ascorbic acid, β-glycerolphosphate, and dexamethasone [68, 69]. The osteogenic potential can be determined by examining alkaline phosphatase (ALP) activity, expression of the osteogenic markers such as osteocalcin, osteocalcin, bone morphogenetic protein, and type I collagen at the mRNA and protein levels, and formation of mineralized ECM containing hydroxyapatite [69, 70].

The required properties of bone tissue scaffolds are biodegradability, porosity that allows cell in-growth, surface properties for cell adhesion and proliferation, osteoinductivity, and sufficient mechanical strength [63]. Generally, ceramics, polymers, and composite of these are being used. Ceramics such as β-tricalcium phosphate, hyaroxyapatite have shown good results regarding bone regeneration due to their osteoconductivity and osteoinductivity [71-74]. However, they are too brittle and their degradation rate is difficult to control [75]. Natural polymers such as collagen [76-78], hyaluronic acid [31, 79-81], and silk [82-84] provide innate biological guidance to cells and exhibit the capability of interacting with the host tissue [75]. Synthetic polymers such as poly(α-hydroxy acids) [85-87] and polycaprolactone [88-91] have chemical versatility and processability, and PEG [92-94] has advantages as hydrogel. However, polymers are too soft and weak. In order to improve the mechanical properties, various ceramics/polymers composite scaffolds [95-99] have also been studied.

1.5. Specific aims of thesis

The goal of this thesis is to develop hydrogels with high mechanical strength and biological activity for tissue engineering applications. There are three chapters in this thesis that describe three separate projects which consistently aimed at developing strong cell-laden hydrogels.

The aim of the first project (Chapter 2) was to synthesize biodegradable, hydrophilic polymer that forms hydrogels with tunable mechanical properties and cell-adhesivity. From two starting monomers, glucose and malic acid, which are found in the human metabolic system, was synthesized the polymer by a polycondensation reaction. By the following modification

with methacrylate groups, the polymer became photocrosslinkable into hydrogels. By altering the ratio of the starting materials and the degree of methacrylation, several formulations were prepared and then characterized chemically and physically. Degradation, mechanical properties of the resulting hydrogels and cell adhesion and proliferation on them were examined.

The second project (Chapter 3) aimed at developing cell-laden strong hydrogels by using the double-network (DN) approach. It was concluded from the first project that it is better to use biomacromolecules with high molecular weights than to synthesize a polymer from monomers to prepare hydrogels with high mechanical strength. In addition, DN approach can develop hydrogels with higher strength than traditional single-network (SN) hydrogels. Thus, in this project, cell-laden DN hydrogels with high strength were developed from two photocrosslinkable biomacromolecules, gellan gum (GG) and gelatin, by using a cell-compatible two-step photocrosslinking. The mechanical strength of the resulting DN hydrogels was measured and compared with that of SN hydrogels, and the parameters that affect the strength of the DN hydrogels were examined. The viability of the cells encapsulated in DN hydrogels was measured to show the cell-compatibility of the DN formation process.

The aim of the last project (Chapter 4) was to develop cell-laden microgel-reinforced (MR) hydrogels from the same two polymers with the DN hydrogels developed in the previous project, which have better mechanical strength and biological properties in comparison to the DN hydrogels. By incorporating the stiff GG network into gelatin hydrogels as microgels, not as bulk hydrogels as for DN hydrogels, embedding GG networks with higher concentrations led to higher strength of the resulting hydrogels, and stronger cell-hydrogel interaction was possible. The mechanical properties of the MR hydrogels were compared to the DN hydrogels and the gelatin hydrogels with no microgels, and the effect of the formulation on the strength of MR hydrogels was investigated. The metabolic activity and osteogenic behavior of the encapsulated preosteoblasts were examined to prove high potential of the MR hydrogels as tissue scaffolds.

Chapter 2: Cell-adhesive and mechanically tunable glucose-based biodegradable hydrogels

The content of this chapter has been published in the following journal article: Shin H, Nichol JW, Khademhosseini A. Cell-adhesive and mechanically tunable glucose-based biodegradable hydrogels. Acta Biomaterialia 2011;7(1):106-114

2.1. Introduction

Synthetic biodegradable polymers are of great interest for various biomedical applications such as drug delivery and tissue engineering [100]. For many biomedical applications, it is desirable to control the mechanical and biological properties of these materials [101]. Previously, various synthetic biodegradable polymers have been made to improve the properties of biomaterials for various applications [102-109]. However, these polymers are generally hydrophobic greatly limiting the ability to encapsulate cells into the construct. Hydrogels, a class of biomaterials formed from hydrophilic polymers, are attractive for many reasons such as their biocompatibility and the fact that they contain similar water content and mechanical properties as natural tissues [110-112]. In particular, hydrogels from photocrosslinkable polymers can be injected into the body, encapsulate cells uniformly, and enable temporal and spatial control in the fabrication of complex structures [14, 15, 110, 111, 113].

Over the years, a number of synthetic hydrogels have been developed for biomedical applications. Poly(2-hydroxyethyl methacrylate) (PHEMA), poly(N-isopropylacrylamide) (PNIPAAm), poly(vinyl alcohol) (PVA) and their derivatives are vinyl monomer based synthetic polymers that have been studied for applications such as contact lenses, drug delivery, and tissue engineering [114-120]. However, these hydrogels are nondegradable and their vinyl monomers and crosslinking molecules may be toxic [110]. Poly(ethylene glycol) (PEG) is one of the most studied hydrophilic biomaterials and has been approved by the FDA for certain applications. While PEG hydrogels are inert and exhibit low toxicity, they are not biodegradable. To render PEG biodegradable, several methods have been developed such as copolymerization of PEG with biodegradable poly(α-hydroxy esters), such as poly(lactic acid) (PLA) and poly(glycolic acid) (PGA), or with peptides that are enzymatically degradable [121-124]. Recently, a new hydrophilic biodegradable polymer, poly(xylitol citrate)methacrylate (PXCma) was

synthesized from non-toxic starting monomers: xylitol and citric acid [108]. While the PEG based hydrogels include PEG macromers in their degradation products, PXCma hydrogels completely degrade into the original monomers, xylitol and citric acid that are endogenous to human metabolic system. However, despite its merits, PXCma was mechanically weak and not cell adherent.

In this study, we synthesized a hydrophilic biodegradable polymer, designated poly(glucose malate)methacrylate (PGMma), which can form hydrogels that degrade into the starting monomers, glucose and malic acid. Glucose is a metabolic intermediate, which is commonly available, inexpensive and could be used as an energy resource by cells when released through degradation of the polymer. Malic acid is nontoxic, an ingredient in many foods and its anion is an intermediate in the citric acid cycle [125]. The polymer form, poly(malic acid), has been demonstrated in various biomedical applications [126, 127]. As in previous reports on using polycondensation reactions with multifunctional monomer(s) to synthesize biodegradable elastomers or hydrogels, we used two hydrophilic, multifunctional monomers, glucose and malic acid, to form a randomly branched, hydrophilic, and hydrolyzable polyester, poly(glucose malate) (PGM) by polycondensation [102, 103, 108, 109]. After the polycondensation reaction, the remaining unreacted hydroxyl groups enabled further functionalization. To render the PGM photocrosslinkable, we functionalized the free hydroxyl groups of PGM with methacrylate groups by reacting PGM with methacrylic anhydride, as previously described for methacrylation of hyaluronic acid [128, 129]. Finally, we used the resulting photocrosslinkable PGMma to fabricate hydrogels through a light initiated crosslinking process. We characterized the properties of the resulting hydrogel as a function of the stoichiometric ratio of the starting monomers, the degree of methacrylation, and polymer concentration. Furthermore, cell adhesion tests showed that PGMma is cell-adhesive. Given its broad range of properties, PGMma may be useful for various tissue engineering applications or as a material in cell culture.

2.2. Materials and methods

2.2.1. Synthesis of PGMma polymers

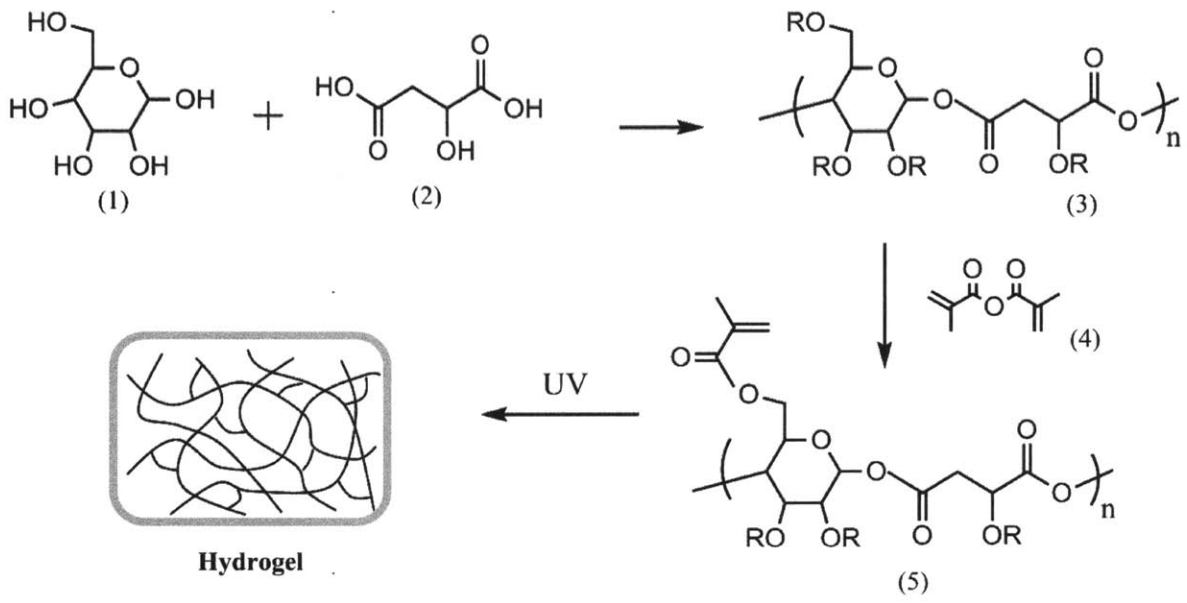

Figure 2.1. General synthetic scheme of PGMma hydrogel. (1) glucose, (2) malic acid, (3) PGM, (4) methacrylic anhydride, (5) PGMma. PGM and PGMma is randomly branched polymer because R can be H, glucose, malic acid, or polymer chain.

All chemicals were obtained from Sigma-Aldrich. PGMma was synthesized as follows (Figure 2.1.). Two batches of PGMs with varying molar ratios of starting materials were synthesized. D-(+)-glucose and DL-malic acid were mixed in a round bottom flask with molar ratio of 1:1 for PGM1:1 and 1:2 for PGM1:2. They were heated and stirred under argon gas to 135°C. Under these conditions, malic acid melts and dissolves the glucose in the mixture. After glucose dissolved completely, vacuum was applied for five minutes and the resulting viscous intermediate material was cured at 90°C for 2 days inside a vacuum oven. The resulting mixture was dissolved in distilled water, dialyzed by a membrane with molecular weight cutoff of 6-8 kD, and lyophilized. PGM macromers were methacrylated as previously described [129]. Briefly, methacrylic anhydride was reacted with PGM in distilled water on ice for 24 h. The pH of the solution was kept at 8 with 5 N NaOH. The solution was then dialyzed (MW cutoff 6k-8kDa) for 48 h, and lyophilized to yield PGMma. To modify the degree of methacrylation (DM), we added varying amounts of methacrylic anhydride (i.e. 1ml, 2ml, and 4ml per 1g of PGM).

2.2.2. Characterization of PGMma polymers

^{1}H-NMR spectra of PGM and PGMma polymers were obtained in D_2O on a Varian 300 NMR spectrometer. The chemical composition of the polymers was calculated by the signal integrals of glucose, malic acid and methacrylate group. Molar ratio of glucose and malic acid in the polymers were calculated by the peaks at 3.2-4.5 ppm from glucose compared with peaks at 2.7-3.2 ppm from malic acid. DM was calculated by the peaks at 1.8-2.0 ppm from methacrylate group and the peaks from malic acid. It was defined as the number of methacrylate groups divided by the number of free hydroxyl groups prior to the methacrylation reaction. Since one hydroxyl group is always removed whenever either a glucose or malic acid monomer becomes attached to the PGM polymer, regardless of the location, the total number of free hydroxyl groups in the resulting PGM polymer will not vary based on the degree of branching. Therefore, the number of hydroxyl groups was counted as the number of glucose monomers multiplied by 3 plus the number of malic acid monomers because, regardless of how the polymer is branched, the number of hydroxyl groups in the resulting PGM structure will be the same as the simplified case where each glucose monomer has three remaining hydroxyl groups and each malic acid monomer has one remaining hydroxyl group. FT-IR analysis was performed on a Bruker Alpha FT-IR spectrometer. Molecular weight distribution was determined by gel permeation chromatography (GPC, Viscotek TDAmax) using PEG standard, 0.05M $NaNO_3$ aqueous solution as eluentia and a 3x Viscotek GPMWxL column with triple detection (refractive index, light scattering, and viscometer detector). By combining the data set obtained from three kinds of detectors, the absolute molecular weight was calculated with high accuracy independent of the degree of branching. Densities of polymers were measured with an Ultrapycnometer 1000 (Quantacrome Instruments).

2.2.3. Photopolymerization

PGMma polymer solutions were prepared by dissolving PGMma polymers at three different concentrations (10, 15, 20 wt%) in phosphate buffered saline (PBS) containing 0.05 wt% photoinitiator (Irgacure 2959). They were subsequently molded into disks (~8mm diameter,

~1mm thickness) and cured by exposure to light (320-500nm, ~4 mW cm^{-2} for 10min) (EXFO OmniCure S2000).

2.2.4. Hydrogel Characterization

Sol content was determined by measuring the difference in mass of dried sample before (m_i) and after (m_f) immersion in distilled water with agitation for 1 h. It was calculated as:

$$\text{Sol content (\%)} = \frac{m_i - m_f}{m_i} \times 100 \quad (1)$$

Hydration by mass was determined by measuring the difference in mass of sol-free hydrogels in relaxed state(m_r) and in swollen state(m_s) after 24 h in PBS. m_r was calculated by measuring the initial mass of hydrogel and subtracting sol content from it. Hydration by mass was calculated as:

$$\text{Hydration by mass (\%)} = \frac{m_s - m_r}{m_r} \times 100 \quad (2)$$

Crosslink density ($n = \rho / M_c$) and molecular weight between crosslinks (M_c) were calculated by the following equation for hydrogels [111]:

$$\tau = \frac{\rho RT}{M_c}(1 - \frac{2M_c}{M_n})(a - \frac{1}{a^2})(\frac{v_s}{v_r})^{\frac{1}{3}} \quad (3)$$

where τ is the compression modulus of the hydrogel, R is the universal gas constant, T is temperature, ρ is the mass density, v_s is the polymer volume fraction in the swollen state, v_r is the polymer volume fraction in the relaxed state, and a is the elongation ratio, which is related to the polymer volume fraction in the swollen state for isotropically swollen hydrogel:

$$a = v_s^{-\frac{1}{3}} \quad (4)$$

Compression analysis of PGMma hydrogels was performed on an Instron 5542 mechanical tester. Hydrogel disks were prepared as described above and allowed to equilibrate in PBS for 24 h and then were compressed on the tester until failure at a rate of 0.2 mm min^{-1}.

Compressive modulus was determined as the slope of the linear region in the 5-10 % strain range.

To analyze the degradation rate of the hydrogels, disks were fabricated as described above and incubated in PBS at 37°C on an orbital shaker. PBS was replaced every 48 h. At each time point, samples were removed, lyophilized and weighed. Mass remaining was calculated by dried mass at each time point (m_t) compared to initial dried mass (m_0) using the following equation:

$$\text{Mass remaining (\%)} = \frac{m_t}{m_0} \times 100 \quad (5)$$

When the hydrogel dissociated completely, we plotted this point as zero mass remaining. Thus the final time point signified in the degradation plot (Figure 2.5) occurred somewhat sooner than the true point at which mass would be actually zero.

2.2.5. Cell culture

NIH 3T3 fibroblasts were cultured in high glucose Dulbecco's Modified Eagle Medium (DMEM, Invitrogen) supplemented with 10% fetal bovine serum (FBS, Invitrogen), 100 U/ml penicillin (Invitrogen), and 100 µg/ml streptomycin (Invitrogen) in a 5% CO_2 atmosphere at 37°C. Cells were passaged approximately 2 times per week and media was exchanged every 2 days.

2.2.6. Cell adhesion and proliferation on PGMma hydrogels

Square hydrogel pieces (1cm × 1cm × 300µm) were made by crosslinking 15% (w/v) PGMma polymer in PBS, which was previously filtered through a 0.2µm filter for sterilization, on 3-(trimethoxysilyl)propyl methacrylate coated glass slides to prevent the gels from detaching from the glass slide in growth media. After soaking the gels in growth media for six hours, they were put in 4-well plates and each well of the plates was filled with 4ml of cell suspension containing 5×10^5 cells ml^{-1}. These plates were then incubated at 37°C and the hydrogel surfaces were imaged at days 1, 2 and 3. To assess viability, cells were stained with live/dead

viability kit (Invitrogen) and visualized under a fluorescent microscope. Confluence of the cells on the hydrogel films were determined by analyzing fluorescent images by using ImageJ software. Three formulations of PGMma – PGMma1:1 medium DM, PGMma1:1 high DM, and PGMma1:2 medium DM - were tested with poly(ethylene glycol) diacrylate 4000 (PEGDA4000, molecular weight: 4000) for comparison. In addition, to test the addition of gelatin for enhancing biological properties of the gels, hydrogels were made by mixing gelatin methacrylamide (GelMA) with PGMma1:2 medium DM (15% PGMma1:2 medium DM + 1% GelMA). Since gelatin is processed from collagen, it contains similar bioactive features as collagen[130]. GelMA was prepared according to a method previously described [131]. To better show the cell morphology, cells cultured on PEGDA4000 and PGMma1:1 medium DM were fixed and stained with Alexa Fluor 594-labelled phalloidin (Invitrogen) and DAPI to visualize F-actin filaments and cell nuclei respectively. Total cell number was quantified by counting DAPI stained nuclei.

2.2.6. Statistical analysis

All data are expressed as mean ± standard deviation. Statistical significance was measured by performing one-way or two-way ANOVA where appropriate (GraphPad Prism 5.02, GraphPad Software). Tukey's multiple comparison test and Bonferroni test were used with one-way and two-way ANOVA each to determine significance between specific treatments. Differences were taken to be significant for $p<0.05$.

2.3. Results

2.3.1. PGMma polymer synthesis and characterization

To generate a hydrogel, we first synthesized the PGM polymer through bulk polycondensation reaction of D-(+)-glucose and DL-malic acid. Since every hydroxyl group of

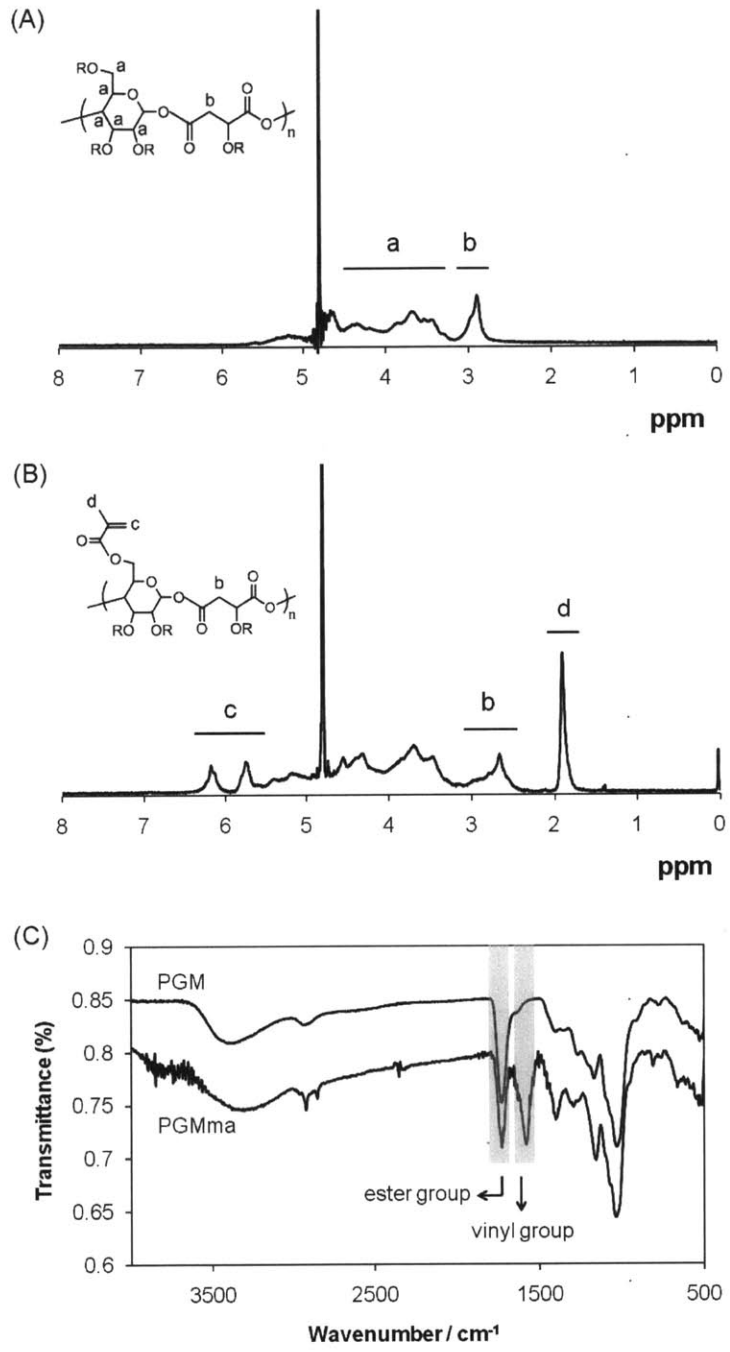

Figure 2.2. (A) Representative ^{1}H NMR spectrum of PGM. (B) Representative ^{1}H NMR spectrum of PGMma. (C) Representative FT-IR spectra of PGM and PGMma.

glucose and malic acid can react, the PGM polymer is randomly branched rather than linear (Figure 2.1. (3)). Two stoichiometric ratios of glucose to malic acid were made: PGM1:1 and

PGM1:2. Figure 2.2. (A) shows a representative ^{1}H NMR spectrum of PGM1:1. The chemical composition of these two PGMs were determined by ^{1}H NMR to be 1 : 1.01 and 1 : 1.97 (Table 1) as determined by the signal integral of glucose and malic acid. These chemical compositions were similar to the molar ratio of the starting materials. An FT-IR spectrum of PGM (Figure 2.2. (C)) confirmed ester bond formation with a peak at 1732cm^{-1}. A broad band centered at 3388cm^{-1} was also detectable, most likely due to hydrogen bonded hydroxyl groups, while a small band centered at 2934cm^{-1} was detectable due to sp^3-hybridized C-H bonds. The number average molecular weight (M_n), weight average molecular weight (M_w), and polydispersity index (PDI) determined by GPC with three types of detectors (refractive index, light scattering, and viscometer detector) are summarized in Table 2.1.

Polymer	Composition by ^{1}H NMR	M_n (×10^4) / g mol^{-1}	M_w (×10^4) / g mol^{-1}	PDI
PGM1:1	1 : 1.01	1.51	9.77	6.5
PGM1:2	1 : 1.97	1.18	6.41	5.4

Table 2.1. Composition by ^{1}H NMR and molecular weight distribution of PGM.

Polymer	Amount of methacrylic anhydride added per 1g of PGM / ml	Degree of methacrylation (%)
PGMma1:1 low DM	1	16
PGMma1:1 medium DM	2	28
PGMma1:1 high DM	4	44
PGMma1:2 low DM	2	23
PGMma1:2 medium DM	4	28

Table 2.2. The amount of methacrylic anhydride added to PGM and the resulting degree of methacrylation of PGMma polymers.

Following polymerization of PGM, methacrylation was performed as described above to obtain PGMma. To achieve differences in DM, we systematically varied the amount of

methacrylic anhydride added to the reaction. The amount of methacrylic anhydride added and DM of each PGMma polymer determined by ^{1}H NMR spectra (representative image in Figure 2.2. (B)) are summarized in Table 2.2. Low (16%), medium (28%), and high (44%) DM were obtained for PGMma1:1, and low (23%) and medium (28%) DM were obtained for PGMma1:2. A representative FT-IR spectrum of PGMma also confirmed methacrylation with a peak due to vinyl groups at 1596cm^{-1}. Average molecular weight and distribution determined using GPC and density measured with a pycnometer are summarized in Table 2.3.

Polymer	M_n ($\times 10^4$) / g mol^{-1}	M_w ($\times 10^4$) / g mol^{-1}	PDI	Density of polymer / g cm^{-3}	Crosslink density / mol m^{-3}	Molecular weight between crosslinks ($\times 10^3$) / g mol^{-1}
PGMma1:1 low DM	1.01	2.58	2.5	1.98±0.02	391	5.06
PGMma1:1 medium DM	0.94	2.05	2.2	1.96±0.06	423	4.64
PGMma1:1 high DM	0.83	1.87	2.2	1.98±0.08	496	3.99
PGMma1:2 low DM	1.14	2.27	2.0	1.85±0.01	324	5.71
PGMma1:2 medium DM	0.96	1.99	2.1	2.01±0.04	435	4.61

Table 2.3. Physical properties of PGMma polymers and hydrogels. Crosslink density and molecular weight between crosslinks were calculated for 15% hydrogels.

2.3.2. Characterization of PGMma hydrogels

Physical properties were measured to characterize the resulting PGMma hydrogels. To measure the amount of the soluble fraction, including microgels that could diffuse out of the gel following crosslinking, the sol content of 15% (w/v) hydrogel of all formulations of PGMma polymers and PEGDA4000 was determined as described above. For PGMma1:1 medium DM, the sol content of 10% and 20% (w/v) hydrogels was measured as well. As seen in Figure 2.3. (A), as DM increased, sol content decreased. PGMma1:1 low DM exhibited the highest sol content, 29.6 ± 0.5%, while PGMma1:1 high DM exhibited the lowest sol content, 5.8 ± 1.1%. Sol content of the lowest DM hydrogel (PGMma1:1 low DM) was similar ($p<0.05$) to that of PEGDA4000. However, the polymer concentration in the hydrogel did not affect the sol content. The difference in sol content for different polymer concentrations in the hydrogel was not

significant ($p<0.05$) (Figure 2.3. (B)). Hydration by mass of sol-free PGMma hydrogels are summarized in Figure 2.3. (C) and (D). Hydration was also measured for 15% (w/v) hydrogel of every formulation of PGMma, in addition to 10% and 20% (w/v) for PGMma1:1 medium DM. As expected, as DM increased, hydration decreased. Among all the formulations, PGMma1:2 medium DM exhibited the highest hydration, 114.1 ± 1.3%, while PGMma1:2 low DM exhibited the lowest hydration, 18.7 ± 0.5%. With respect to the concentration, the 20% hydrogel exhibited higher hydration than the other two concentrations, however, the difference between 15% and 20% hydrogels was not significant ($p<0.05$).

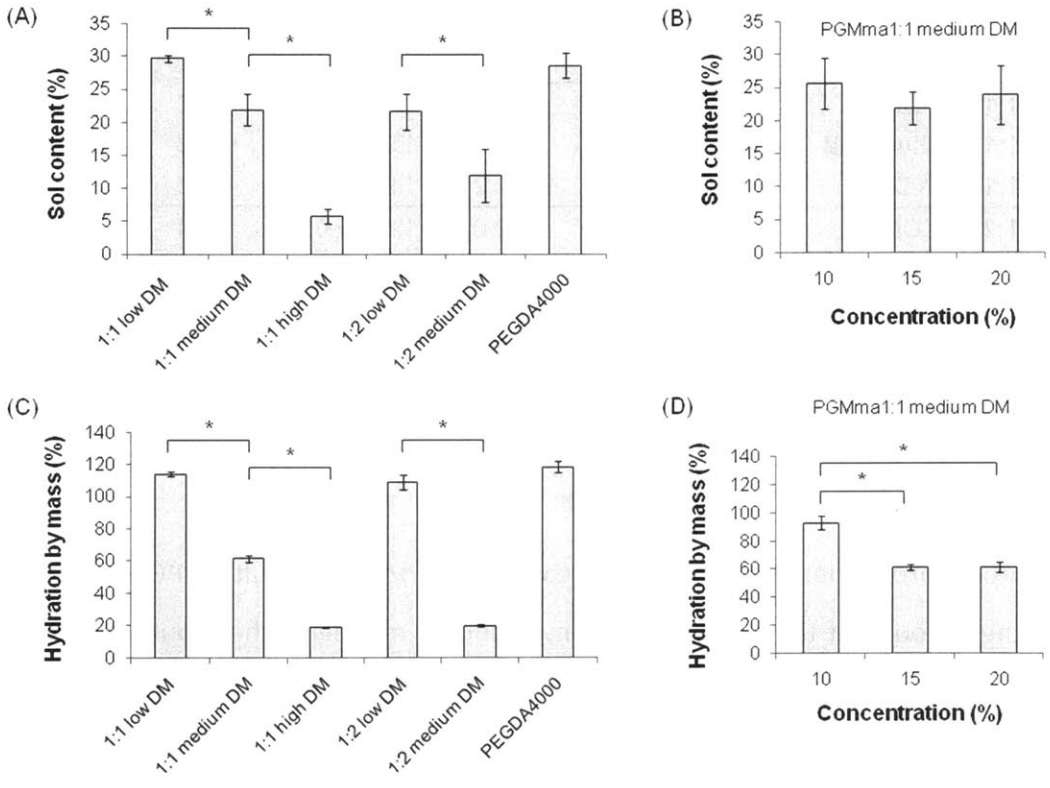

Figure 2.3. Sol content of (A) 15% (w/v) hydrogels of each PGMma formulation compared with PEGDA4000, and (B) PGMma1:1 medium DM hydrogels with different concentrations. Hydration by mass of (C) 15% (w/v) hydrogels of each PGMma formulation compared with PEGDA4000, and (D) PGMma1:1 medium DM hydrogels with different concentrations. (*) indicates significant difference ($p<0.05$).

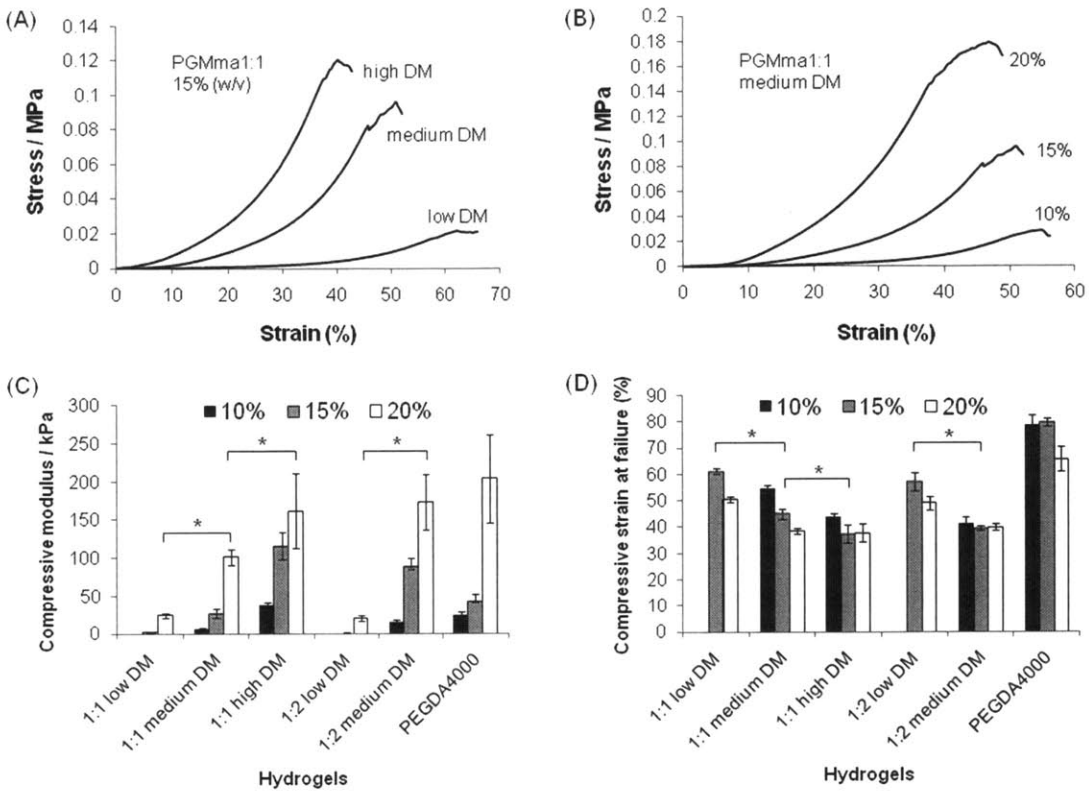

Figure 2.4. Stress-strain curve of PGMma1:1 hydrogels (A) 15%(w/v) of each DM, (B) different polymer concentrations (10%, 15%, 20% (w/v)) of medium DM. (C) Compressive modulus of PGMma1:1 and PGMma1:2 hydrogels compared with that of PEGDA4000 hydrogel. (D) Compressive strain at failure of PGMma1:1 and PGMma1:2 hydrogels compared with that of PEGDA4000 hydrogel. (*) indicates significant difference ($p<0.05$).

To characterize the mechanical properties of PGMma hydrogels, compression analysis was performed using unconfined, uniaxial compression. Figure 2.4. (A) shows representative stress-strain curves of PGMma1:1 15% hydrogels with varying DM (low, medium, high), while panel (B) shows representative stress-strain curves of PGMma1:1 medium DM hydrogel with varying polymer concentration (10%, 15%, 20% (w/v)). Compressive modulus and compressive strain at failure of all formulations of PGMma hydrogels measured are shown in Figure 2.4. (C) and (D) together with those of 15% polymer concentration PEGDA4000 hydrogel for comparison. For both PGMma1:1 and PGMma1:2 with low DM, hydrogels could not be made from 10% polymer solution. Overall, the compressive modulus increased as DM increased or polymer concentration increased. For example, 15% hydrogels of PGMma1:2 low DM exhibited

a compressive modulus of 1.8 ± 0.4kPa, while 20% hydrogels of PGMma1:2 medium DM exhibited a modulus of 172.7 ± 36kPa. The compressive modulus of both PGMma1:1 high DM and PGMma1:2 medium DM was comparable to that of PEGDA4000. The compressive strain at failure generally decreased as DM increased or polymer concentration increased. However, the difference was not as great as that seen with the compressive modulus. For example, the compressive strain at failure of 15% PGMma1:1 high DM was not significantly different from that of the 20% hydrogel of the same polymer ($p<0.05$). The compressive strain at failure of PGMma hydrogels ranged from 37.5 ± 0.9% to 61.2 ± 1.1%, which shows PGMma was not as compressible as PEGDA4000, which exhibited compressive strain at failure values ranging from 65.7 ± 6.7% to 79.6 ± 1.6%.

2.3.3. In vitro degradation of PGMma hydrogels

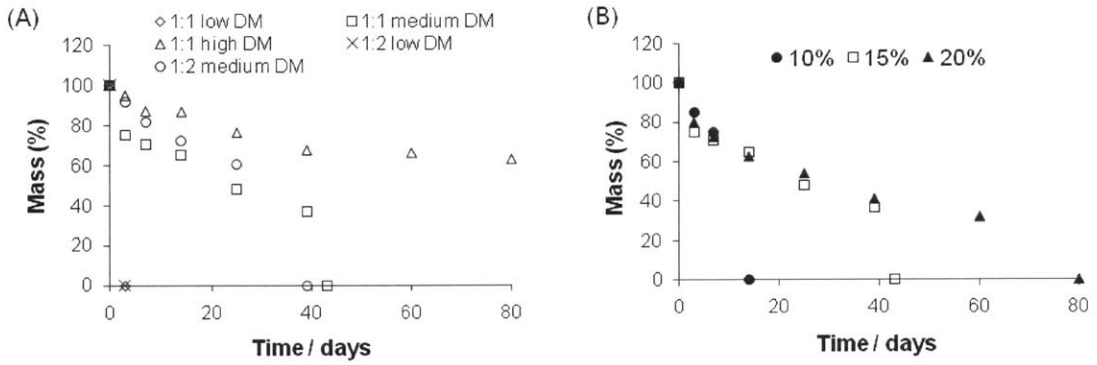

Figure 2.5. Mass-loss over time of PGMma hydrogels in PBS at 37°C (A) 15% (w/v) of each formulation, (B) PGMma1:1 medium DM.

PGMma hydrogels were hydrolytically degradable in PBS (Figure 2.5). As shown in Figure 2.5. (A), PGMma polymers exhibited a broad range of degradation rates. For example, hydrogels with a low DM dissociated in 3 days, whereas those with high DM showed a much slower degradation rate (at least 80 days). The degradation rates of PGMma1:1 medium DM hydrogels with varying polymer concentrations (10%, 15%, 20% (w/v)) are shown in (B). Interestingly, the initial degradation rates were similar for all concentrations, however, at a

critical point, the hydrogels dissociated abruptly. This critical time occurred sooner for hydrogels with lower polymer concentrations. For example, 10% hydrogels dissociated by day 14, while 15% hydrogels dissociated by day 43, and 20% hydrogels did not dissociate throughout the 80 day study.

2.3.4. Cell adhesion and proliferation on PGMma hydrogels

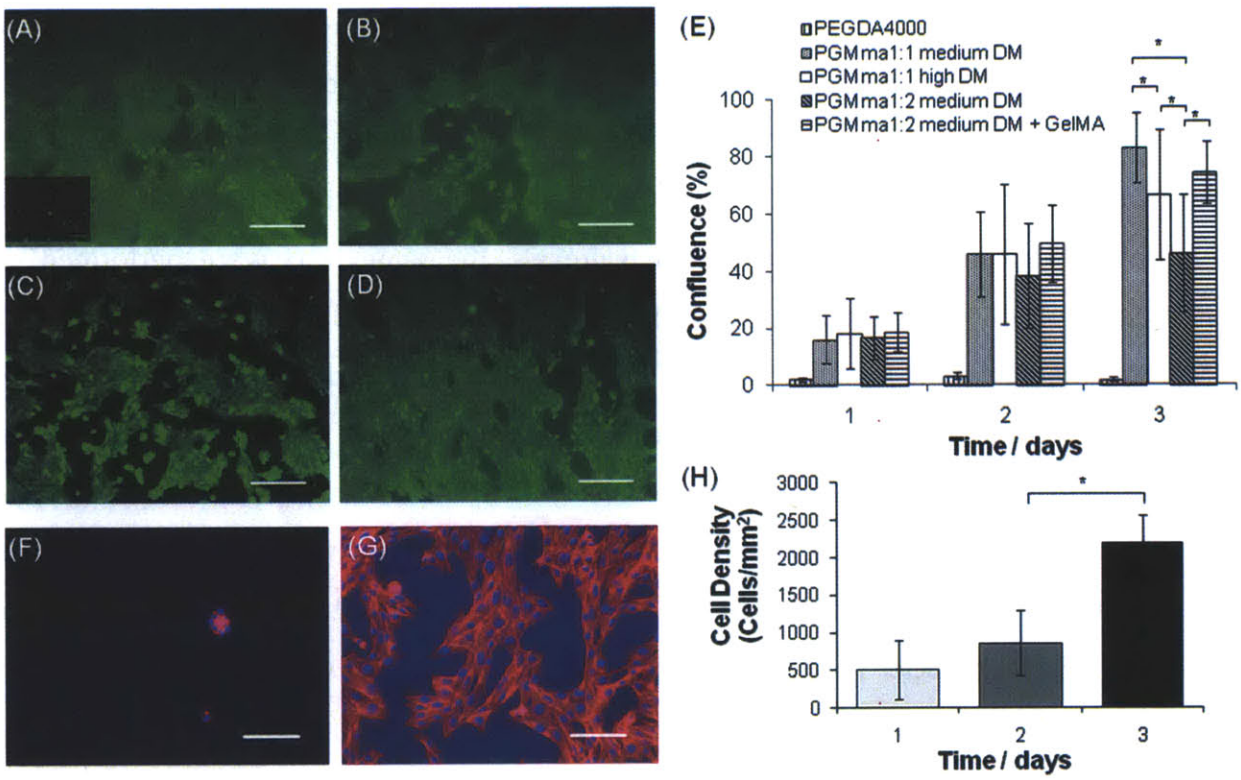

Figure 2.6. Fluorescence images (10x) of live/dead stained 3T3 fibroblasts after 3 days of culture on PEGDA4000 (inset in (A)), (A) PGMma1:1 medium DM, (B) PGMma1:1 high DM, (C) PGMma1:2 medium DM, and (D) PGMma1:2 medium DM + GelMA. The polymer concentration of hydrogels is 15% (w/v). Bars represent 200μm. (E) Attachment and proliferation of 3T3 fibroblasts on different hydrogels. (*) indicates significant difference ($p<0.05$) to the other hydrogel(s) for that time point. Phalloidin/DAPI staining for F-actin/cell nuclei on day 2 of culture on (F) PEGDA4000 and (G) PGMma1:1 medium DM. Scale bars represent 100μm. (H) Determination of cell density, defined as the number of DAPI stained nuclei per PGMma1:1 medium DM hydrogel area. (*) indicates significant difference ($p<0.05$).

To determine the adhesivity of the PGMma hydrogels, the initial attachment and subsequent proliferation of 3T3-fibroblasts on three formulations of PGMma hydrogels was compared to PEGDA4000 (Figure 2.6). Consistent with previously published reports, cells did not significantly adhere to PEGDA4000 [132, 133]. Interestingly however, cells readily attached to and spread on all PGMma hydrogels. The levels of initial cell attachment as measured by the extent of confluence at day 1 were similar for all glucose-based hydrogels tested ($p<0.05$). To analyze cell proliferation, cell-seeded hydrogels were cultured for 3 days. We observed that after 2 days, cells proliferated on all PGMma hydrogels and there was no significant difference in the level of confluence among PGMma hydrogels. However, after 3 days, differences in proliferation were seen among PGMma hydrogels. At this time, the confluence on PGMma1:1 medium DM was the highest while that on PGMma1:2 medium DM was the lowest ($p<0.05$) among the three formulations of PGMma. To assess the effect of the addition of GelMA on enhancing biological properties of PGMma hydrogels, the same tests were performed on GelMA-added PGMma1:2 medium DM and the data was compared with that of pure PGMma1:2 medium DM. In these studies, the extent of cell attachment at day 1 and the confluence at day 2 was not significantly different. However at day 3, GelMA-added PGMma1:2 medium DM exhibited significantly higher confluence than the same hydrogels without GelMA ($p<0.05$). To better demonstrate cell morphology and changes in the total cell number over time, we stained the cells cultured on PEGDA4000 and PGMma1:1 medium DM for F-actin (phalloidin) and cell nuclei (DAPI). The cells on PGMma1:1 medium DM hydrogels clearly exhibited spread morphology, and the cell density increased significantly by day 3 ($p<0.05$).

2.4. Discussion

The melting point of D-(+)-glucose and DL-malic acid are 150-152°C and 131-133°C, respectively. Once the glucose begins to melt at temperatures above 150°C, it starts to caramelize by a browning reaction due to oxidation. Therefore, the first polycondensation step to synthesize PGM, which involves heating and curing, was done at 135°C and 90°C to minimize this effect. To do this, glucose was dissolved into liquid malic acid, instead of melting the glucose and malic acid mixture above 150°C. Despite this reduced reaction temperature,

glucose and malic acid reacted thoroughly to yield a polyester material, PGM, which was confirmed by GPC, FT-IR and ^{1}H-NMR analysis. Furthermore, the chemical composition of PGM, as determined by ^{1}H-NMR, correlated well to the initial molar ratios of glucose and malic acid. Even though the multiple hydroxyl groups in glucose and one in malic acid make PGM polymers structurally heterogeneous, the remaining unreacted hydroxyl groups following polycondensation enable PGM to be water-soluble, which is one of the critical reasons that glucose was chosen as a starting material. Glucose can exist either in the ring form with no aldehyde groups, or in the open-chain form containing an aldehyde group [134]. Since the ^{1}H NMR spectrum of PGM does not contain a peak indicative of the aldehyde groups, we conclude that the majority of the glucose in PGM remained in the ring form.

There were differences in the reaction characteristics for methacrylation of the different PGM polymers. For example, it was more difficult to methacrylate PGM1:2 than it was for PGM1:1 (Table 2). When 2 ml of methacrylic anhydride per 1 g of PGM was added, the DM of PGMma1:1 was 28%, whereas the DM of PGMma1:2 was 23%. By doubling the amount of methacrylic anhydride, the DM of PGMma1:1 was increased to 44%, whereas the DM was only increased to 28% for PGMma1:2. This is likely due to the presence of more unreacted hydroxyl groups which are available for methacrylation in PGMma1:1 as compared to the PGMma1:2 polymers. Another possible explanation is that PGM1:2 is more branched than PGM1:1 so methacrylate groups cannot access the free hydroxyl groups in PGM1:2 as easily as is possible in PGM1:1. It appeared from Table 1 and 2 that methacrylation resulted in a decrease in both the molecular weight and PDI, and as DM increased, the molecular weight decreased. The ester bonds of PGM can be hydrolyzed in aqueous solution, particularly faster in either acidic or basic conditions. Since the methacrylation is done in a weak basic aqueous solution, some hydrolysis likely occurred to decrease the molecular weight of the resultant PGMma. If the molecular weight is larger, the chance of hydrolysis in the macromer is higher, and small macromers were removed by dialysis. These are likely to be the reasons that PDI decreased. The reason that as DM increased, molecular weight decreased is likely to be that increased methacrylic acid derived from methacrylic anhydride and sodium hydroxide which was added to keep the pH

constant, led to increased hydrolysis of ester bonds. In addition, more methacrylic anhydride remained after the 24h reaction leading to some continued hydrolysis during the dialysis step.

The control or repeatability of the synthesis is important because if the structure, such as degree of branching, of the material varies, the properties of hydrogels are likely to be different. Therefore, tight adherence to the protocols would be required to avoid significant batch to batch variation. As the number of remaining hydroxyl groups after the polycondensation reaction does not vary according to the degree of branching, unless there is a big difference in the degree of branching and thus a big difference in the accessibility of the remaining hydroxyl groups, DM would not be much different from batch to batch and neither would be the mechanical properties of the hydrogels. If the methacrylation process were automated to input NaOH as needed according to the instantaneous pH, the material could be synthesized much more consistently for potential applications.

As expected, the sol content decreased as DM increased in PGMma hydrogels (Figure 2.3. (A)). This is because as DM increases and crosslinking increases, the amount of soluble polymer chains remaining in the gel decreases. Interestingly, there was no significant change in sol content as a function of polymer concentration changes in the hydrogels (Figure 2.3. (B)). This indicates that at least in this concentration range, the concentration increase does not result in more propagation of crosslinking in the hydrogels. A state of equilibrium hydration is reached in which two opposing driving forces of an elastic retractive force by polymer networks and a diluting force related to the enthalpy and entropy of mixing are balanced [135]. Although the PGMma1:2 polymer exhibited a narrower range of DM (23% (low) and 28% (medium)) compared to that of PGMma1:1 (16% (low), 28% (medium), 44% (high)), they displayed a comparable range of hydration by mass (Figure 2.3. (C)) to that of PGMma1:1. This could be explained by the difference in the hydrophilicity of glucose and malic acid, the accessibility to vinyl groups during crosslinking, and the network structure of PGMma1:1 and PGMma1:2. As shown in Figure 2.3. (D), hydration did not decrease substantially when the polymer concentration increased from 15% to 20%. In this case, the concentration change did not lead to a significant change in the balance of the diluting force and the retractive force.

For potential tissue engineering applications, matching the mechanical properties of the polymer scaffold with those of the natural tissues is desirable [136]. The compressive modulus of PGMma hydrogels varied from 1.8 ± 0.4kPa to 172.7 ± 36kPa (Figure 2.4.) which is in the range of moduli for many natural tissues. For example, human relaxed (6kPa) and contracted smooth muscle (10kPa), human carotid artery (84 ± 22kPa), rat skeletal muscle (100kPa), human spinal cord (89kPa), mouse cardiac muscle (20-150kPa), human thyroid (9kPa), and guinea pig lung (5-6kPa) have moduli in this range [136, 137]. As shown in equation (3), the molecular weight (M_n) of the polymer has a great influence on the resulting moduli of hydrogel. Thus, increasing the average molecular weight of PGMma could be a potential method to increase the stiffness of PGMma hydrogels. In addition, PGMma is a branched polymer before it forms a hydrogel, so the degree of entanglement in the polymer solution and in the hydrogel would be reduced. This could explain why PEGDA4000 hydrogels were as stiff as PGMma gels with a high DM. Thus, developing a synthesis method to make linear PGMma-like polymers could be useful in creating hydrogels with greater stiffness. Given the range of DM values obtained and the molecular weight between crosslinks (Table 2) calculated by using equation (3), it is likely that a major fraction of the acrylic moieties react with each other to make only local links so they do not greatly affect the modulus of the hydrogels. Only a minor fraction of the acrylic moieties are being reticulated.

Within the PGMma hydrogels, ester bonds can undergo hydrolysis to induce bulk degradation, where the material degrades throughout its entire volume at the same time [138]. PGMma gels degraded more quickly than hydrophobic polyester biopolymers many of which undergo surface-erosion degradation, where degradation occurs only at the surface [103, 108, 109]. As expected, the DM, which is related to the crosslinking density, was responsible for altering the degradation rate, so as the DM increased, the degradation rate decreased. However, the effect of polymer concentration on the degradation rate behaved differently. Until the point at which hydrogels dissociated, hydrogels of different polymer concentrations displayed similar degradation rates. The time at which hydrogels dissociated completely came earlier for hydrogels at lower polymer concentrations. This indicates that the crosslinking density did not vary significantly with the concentration change. However, there is an absolute quantity of

polymer that is necessary to preserve hydrogel shape, causing a decrease in time for lower concentration hydrogels to dissociate completely due to bulk degradation. This degradation data was obtained without washing the gels with distilled water before freeze drying because at times the gels were too fragile to withstand washing. Thus, salts in the PBS may have contributed to the dry weight of the gels causing the remaining mass to be slightly overestimated. However, although the absolute value of actual remaining mass could be slightly different from the presented data, the trend of lower DM PGMma degrading faster than higher DM PGMma will be preserved. In the case of different concentrations in Figure 2.5. (B), since the hydration by mass of 15% and 20% gels is similar, the trend of these two having similar degradation rates until the point of dissociation is not likely to change. In addition, the time needed for dissociation is not affected by the effect of salts.

Since PGMma is hydrophilic and does not contain known cell-adhesive motifs, we anticipated that cells would not attach onto PGMma hydrogels. However, we found that after soaking the gels in cell culture media for 6 hrs, PGMma gels were cell adhesive (Figure 6). These hydrogels displayed significantly greater cell attachment as compared to PEGDA4000 which was treated in the same manner. This may be due to adsorption of a layer of adhesive proteins from the serum onto PGMma hydrogels, however this was not confirmed. This protein adsorption is possible because PGMma has a greater quantity of hydrophobic methacrylate groups than PEGDA, which only has acrylate groups at the ends of each PEG molecule. In addition, by comparing PGMma1:2 medium DM with and without co-polymerized GelMA, we concluded that GelMA appeared to improve cell proliferation on the PGMma hydrogel surface. Through simple mixing of GelMA with PGMma, the biological properties of PGMma hydrogels could be easily tuned. This demonstrates that it is possible to improve the biological properties of PGMma hydrogels through incorporation of bioactive materials such as RGD motifs. Since the amount of GelMA mixed into hydrogels was small (1%) compared to that of PGMma (15%), and GelMA hydrogels are less stiff than PGMma hydrogels [139], the inclusion of GelMA into PGMma hydrogels is not likely to greatly affect the resultant mechanical properties of the composite hydrogel. However, if greater quantities of GelMA were used, this would have to be considered.

PGMma hydrogels degrade into glucose, malic acid, and a group of molecules derived from reacted methacrylate groups. Glucose could be used as an energy source for cells, which is likely to be useful in tissue engineering applications although the overall scaffold size should be carefully considered to avoid unsafe glucose levels in certain patients, such as those with diabetes.. However, high concentrations of malic acid released from the gels could be harmful to cells due to its acidity if the hydrogels degrade rapidly. Thus, addition of other materials to offset the acidity of the malic acid, or use of slow degrading formulations could be useful. In addition, as shown in the ^{1}H NMR spectrum of PGMma (Figure 2.2. (B)), the ratio of the amount of methacrylate groups in PGMma is large as compared to other methacrylated natural polymers for biomedical applications [128, 140-142]. Since the potential effect of the molecules derived from methacrylate groups are not well characterized, it is desirable to decrease the needed quantity of methacrylate groups to be able to form hydrogels. This could be achieved by synthesizing polymers with higher molecular weight. Alternatively, chemical modification of the PGM polymer to produce other degradation products could also render PGM applicable to wider range of biomedical applications.

2.5. Conclusions

In this study, we synthesized a hydrophilic, biodegradable polymer, PGMma, from biologically relevant molecules, glucose and malic acid, without the need for organic solvents. This polymer is photocrosslinkable by the incorporation of methacrylate groups that initiate the crosslinking of polymer chains upon exposure to light. We demonstrated that by altering the chemical composition, the degree of methacrylation, and the polymer concentration in the hydrogels, the properties of PGMma polymers and hydrogels could be tuned. PGMma hydrogels were degradable and cell-adhesive. Given their wide range of properties, PGMma hydrogels could be potentially useful for a number of biomedical applications such as scaffolds for tissue engineering or tissue culture.

Chapter 3: The mechanical properties and cytotoxicity of cell-laden double-network hydrogels based on photocrosslinkable gelatin and gellan gum biomacromolecules

The content of this chapter has been published in the following journal article: Shin H, Olsen BD, Khademhosseini A. The mechanical properties and cytotoxicity of cell-laden double-network hydrogels based on photocrosslinkable gelatin and gellan gum biomacromolecules. Biomaterials 2012;33(11):3143-3152

3.1. Introduction

Load-bearing tissues, such as cartilage, tendon, and muscle exhibit high strength and toughness, despite their softness [33, 41]. For example, cartilage frequently takes compressive stress of several MPa, and withstands up to 14-59 MPa without failure [41, 143, 144]. To approximate these mechanical properties, various biomaterials have been developed and studied as artificial soft tissues; however, the large difference between natural tissues and artificial biomaterials still presents a challenge [8, 136, 145].

Hydrogels are promising candidates for tissue engineering scaffolds due to their high water content, high permeability to small molecules, biocompatibility, and mechanical properties which resemble natural tissues [41, 110, 111]. Cells can be encapsulated within hydrogels for cell delivery and three dimensional (3D) cell culture. Such cultures better mimic the natural cellular environment to understand the role of the native microenvironment on cellular functions and tissue formation [15, 146]. However, hydrogels are often too soft and weak to be applied for a number of tissue engineering applications that require extensive load bearing behavior. Therefore, developing hydrogels with high mechanical strength is a critical challenge for expanding the range of applications of hydrogels for tissue engineering scaffolds.

Double-network (DN) hydrogels have attracted a great deal of attention for their high fracture toughness and high fracture stress [47, 49]. They are specialized interpenetrating networks (IPNs) in that they are composed of networks with opposite mechanical properties, which results in high strength. In the case of DN hydrogels, the first network is stiff and brittle whereas the second is soft and ductile. In this scheme, the rigid network sustains the stress throughout the material, and the ductile network dissipates energy near the crack tip, preventing the fracture of gels [51]. Various DN hydrogels from different materials have been

reported [47, 49, 50, 147], however, these previous studies did not attempt to encapsulate cells to make cell-laden 3D tissue constructs due to synthetic conditions for DN formation that were incompatible with cell encapsulation. These include the use of toxic crosslinkers or the long crosslinking time needed for the network formation from small molecules. Normal IPNs prepared from biomacromolecules that can encapsulate cells were developed; however, the fracture stress did not reach to the order of MPa [10].

Photocrosslinking of macromolecules provides a method for hydrogel fabrication that has been demonstrated to be compatible with cell encapsulation [12, 13]. The photocrosslinking method has been used to make hydrogels for many tissue engineering studies by modifying various polymers with photoreactive groups. This approach does not need toxic crosslinkers, allows for injection of polymers into the body without large incisions, and enables temporal and spatial control in the fabrication of complicated structures [14, 15, 110, 113]. Since chemical crosslinks are irreversible, photocrosslinked hydrogels are relatively stiff and stable. However, the heterogeneous distribution of crosslinks in photocrosslinked hydrogels results in concentrated stress around the dense crosslinks, causing the hydrogels to fail at low stress [41]. Typically, the compressive moduli of photocrosslinked hydrogels range up to a few hundreds of kPa, and the failure stresses are on the order of tens to hundreds of kPa at the polymer concentrations of 0.5-20% [40, 128, 148, 149].

In this study, by a two-step photocrosslinking of two modified biomacromolecules, gellan gum methacrylate (GGMA) and gelatin methacrylamide (GelMA), we developed DN hydrogels with high strength that can encapsulate cells. Gellan gum (GG) is a bacterial polysaccharide consisting of a tetrasaccharide repeating unit. GG has been approved by FDA as a food additive and has been recently receiving attention for tissue engineering applications [150-152]. Metharylated GG was created to make stiff hydrogels, and highly methacrylated GG hydrogels were reported to have a modulus of more than 100 kPa at only 1% polymer concentration[148]. Gelatin is denatured collagen, which is a major constituent of the extracellular matrix (ECM). Due to the natural cell binding motifs, such as RGD, gelatin exhibits great biological properties such as cell adhesion and cell elongation, which makes it an attractive material for tissue engineering applications. These two polymers were modified into

photocrosslinkable GGMA and GelMA and fabricated into DN hydrogels. The formation of the DN was examined by diffusion tests of the large GelMA molecules into the GGMA network, measuring the resultant enhancement in the mechanical properties, and comparing the mechanical properties between GGMA/GelMA single networks (SN) and DNs. The mechanical properties of DN hydrogels were also compared with those of each GGMA and GelMA SN hydrogels. The effect of the crosslink density of the second network and the concentration of each component in preparation of DN hydrogels on the mechanical properties of DN hydrogels was studied. Lastly, NIH-3T3 fibroblasts were encapsulated in DN gels and the viability was assessed to demonstrate the cell-compatibility of the whole process of DN network formation.

3.2. Materials and methods

3.2.1. Synthesis of GGMA and GelMA polymers

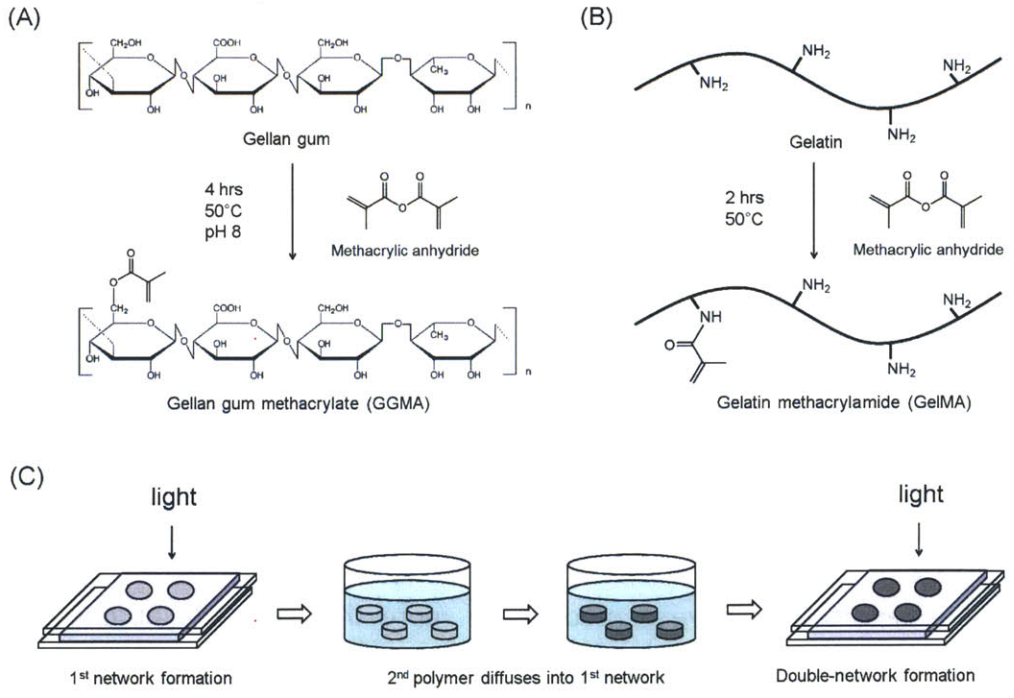

Figure 3.1. Synthesis scheme of (A) gellan gum methacrylate (GGMA) (pictured as above for simplicity, although methacrylic anhydride can react with any hydroxyl group in gellan gum) and (B) gelatin methacrylamide (GelMA). (C) Fabrication of DN hydrogels through a two-step photocrosslinking process.

GG (Gelzan™, Molecular weight: 1,000,000), gelatin (from procine skin, Type A), and methacrylic anhydride were purchased from Sigma-Aldrich. GGMA and GelMA were synthesized by reacting GG and gelatin with methacrylic anhydride (Figure 3.1A-B) [20, 148]. Briefly, 1g of GG was dissolved in 100ml of distilled water at 90°C for 30min, and 8ml of methacrylic anhydride was added at 50°C. The reaction was continued for 4hrs at 50°C while the pH of the solution was maintained at 8 by adding 5N NaOH solution. Then the solution was dialyzed in distilled water using dialysis tubing (molecular weight cutoff: 12-14 kDa, Spectrum Labs, Inc.) at 4°C for 4 days. The solution was lyophilized to obtain pure GGMA, and it was stored at -40°C until further use. Similarly, 20g of gelatin was dissolved in 200ml of phosphate buffered saline (PBS, 1X, Invitrogen) at 50°C, and varying amounts of methacrylic anhydride was added to vary the degree of methacrylation. The reaction was continued for 2hrs at 50°C, and then the solution was dialyzed against distilled water at 40°C for at least 3 days. The solution was lyophilized to obtain pure GelMA, and it was stored at -40°C until further use.

3.2.2. ^{1}H NMR

The degree of methacrylation (DM) of GGMA and GelMA was measured by ^{1}H NMR (Varian Inova 500). GGMA was dissolved in D_2O at 10 mg/ml at 50°C and the spectrum was obtained at 50°C. The DM of GGMA, defined as the number of methacrylate groups attached to GG divided by the number of hydroxyl groups of unreacted GG, was calculated by integrating the peak at 1.5 ppm from the methyl group of the rhamnose unit, and the peak at 2.0 ppm from the methyl group of the methacrylate group [153]. GelMA polymers were dissolved in D_2O at 30 mg/ml at 40°C and the spectra were obtained at 40°C. The DM of GelMA, defined as the number of methacrylate groups attached to gelatin divided by the number of amine groups of unreacted gelatin, was calculated by integrating the peaks at 7.4 ppm from the aromatic residues of gelatin, and the peaks at 5.5 ppm and 5.7 ppm from the double bond hydrogens of methacrylate groups [17, 154].

3.2.3. Fabrication of SN and DN hydrogels

GGMA polymer solutions were prepared by dissolving GGMA polymer at different concentrations (0.5, 1.0, 1.5% (w/v)) at 50°C for 1 day in distilled water containing 0.1% (w/v) photoinitiator, 2-hydroxy-1-[4-(2-hydroxyethoxy)phenyl]-2-methyl-1-propanone (Irgacure 2959, Ciba Specialty Chemicals). The solutions were molded into disks with ~8mm diameter and ~1mm thickness, and exposed to light (320-500 nm, ~7 mW/cm^2, EXFO OmniCure S2000) for crosslinking for varying times. Likewise, GelMA SN hydrogels were fabricated by preparing GelMA polymer solutions at different concentrations at 40°C in distilled water containing 0.1% (w/v) photoinitiator, and crosslinking the solutions in the same manner at 37°C for 120 s. GGMA/GelMA SN hydrogels were fabricated by preparing GGMA/GelMA mixed solutions at different concentrations in distilled water containing 0.1% (w/v) photoinitiator at 50°C for 1 day, and crosslinking the solutions in the same manner at 37°C for 120 s. To fabricate GGMA/GelMA DN hydrogels (Figure 3.1C), GGMA hydrogels were immersed in GelMA solutions (5, 10, 15, 20% (w/v) in distilled water) containing 0.1% (w/v) photoinitiator at 37°C for 2 days on a shaker to allow GelMA molecules to diffuse into GGMA hydrogels. Subsequently, the hydrogels were taken out of the GelMA solutions, and after removing the excess GelMA solutions from the surface of the hydrogels, they were exposed to light again for varying times. All the resulting SN and DN hydrogels were immersed in distilled water at 37°C for 12 hrs and used for further experiments.

3.2.4. Diffusion test

To make fluorescent GelMA polymers, fluorescein isothiocyanate (FITC, Sigma-Aldrich) was conjugated to GelMA polymer based on the manufacturer's instruction. Briefly, 1g of GelMA (DM: 14.7%) was dissolved in 50ml of sodium bicarbonate (Sigma-Aldrich) aqueous solution (100 mM) at 40°C, and 20mg of FITC was dissolved in 10ml dimethyl formamide (DMF, EMD chemicals). The two solutions were mixed and reacted for 6 hrs at 40°C. The resulting solution was dialyzed against distilled water at 40°C for 7 days, and lyophilized to obtain solid FITC-GelMA. The reaction and purification were performed in the dark to minimize fluorescein photobleaching. To examine the diffusion of GelMA molecules into GGMA hydrogels, FITC-GelMA and GelMA (DM: 14.7%) were dissolved together (mass ratio of 1:23) at the

concentration of 20% in distilled water containing 0.1% (w/v) photoinitiator. Previously prepared cylindrical (~8mm diameter, ~1mm thickness) 0.5% GGMA hydrogels were immersed in the solution on a shaker at 37°C. At each time point, the hydrogels were taken out to be exposed to light for 120 s, immersed in distilled water for ~10 mins at 37°C, and cross-sectioned in the middle to be observed under a fluorescence microscope (Nikon TE 2000-U). Relative fluorescence intensity profiles over the thickness of the cross section were plotted by using ImageJ software. The diffusion coefficient of GelMA molecules in GGMA hydrogel was estimated by fitting the fluorescence intensity profiles in the solution to the diffusion equation by using Origin 6.0 software.

3.2.5. Mechanical test

The mechanical properties of hydrogels were measured by unconfined, uniaxial compression tests by using an Instron 5542 mechanical tester. Cylindrical hydrogels were prepared as described above and immersed in distilled water until they reached a swelling equilibrium. They were compressed at a rate of 0.3 mm/min^{-1} until failure. The compressive modulus was determined as the slope of the linear region in the 0-10% strain range of the stress-strain curve. The failure strain and the failure stress were taken from the point where a crack starts to be observed. This happened when the stress-strain curve dropped suddenly or the slope of the curve started to decrease, according to the brittleness of the hydrogels. As it was difficult to identify the failure point in case of GelMA SN hydrogels, the hydrogels were compressed to an ending stress, removed from the tester, and manually checked for cracks while varying the ending stress by 0.5 MPa.

3.2.6. Hydrogel characterization

To determine the fraction of unreacted double bonds in GGMA hydrogels, Fourier transform infrared spectroscopy (FTIR) analysis was performed. To prepare samples for FTIR, 0.5% GGMA hydrogels were fabricated as described above varying crosslinking time from 45s to 360s. The resulting hydrogels were immersed in distilled water and then lyophilized, and the

spectra were taken by a FTIR spectrometer (Bruker Alpha) with an attenuated total reflection (ATR) module.

Water content of hydrogels was determined by measuring the mass of hydrogels in the swollen state and in the dried state. It was calculated as the difference between the mass in the swollen state and that in the dried state divided by the mass in the swollen sate. The mass ratio of each network in DN hydrogels was calculated by using the water content of GGMA SN hydrogels and DN hydrogels.

3.2.7. Cell culture and encapsulation

NIH-3T3 fibroblasts were cultured using Dulbecco's Modified Eagle Medium (DMEM, high glucose, Invitrogen) supplemented with 10% fetal bovine serum (FBS, Invitrogen) and 1% penicillin-streptomycin (Invitrogen) in an atmosphere with 5% of CO_2 at 37°C. Cells were trypsinized and replated every 3-4 days and media was replaced every 2-3 days.

A cell suspension of NIH-3T3 fibroblasts (5×10^6 cells/ml) was prepared by trypsinization and resuspension into the media described above. 1% GGMA solution in distilled water containing 0.2% photoinitiator was also prepared and mixed with the cell suspension at 1:1 volume ratio. The resulting mixture was pipetted on a Petri dish and the mixture drop was covered by a 3-(trimethoxysilyl)propyl methacrylate (TMSPMA)-coated glass slide with two 300 μm spacers between the Petri dish and the glass slide. Subsequently, a photomask with square patterns (900 x 900 μm) was placed on the glass slide and the mixture was exposed to light (320-500 nm, ~7 mW/cm^2) for 120s. The resulting microgels attached to the glass slide were then immersed in previously prepared 20% GelMA (DN:14.7%) solution in media containing 0.1% photoinitiator, and placed on a shaker in an incubator. After 24 hrs, the samples were taken out and exposed to light again for 120s. A calcein AM/ethidium homodimer-1 live/dead assay (Invitrogen) was performed according to the manufacturer's instructions to assess the cell viability in the resulting DN gels following 1 hr (Day 0) and 3 days of culture in media. Similarly, NIH-3T3 fibroblasts were encapsulated in each 0.5% GGMA and 20% GelMA SN hydrogels, and the live/dead assay was performed at day 0 and day 3.

3.2.8. Statistics

All data were expressed as mean ± standard deviation. T-test, one-way, or two-way ANOVA followed by Tukey's test or Bonferroni test was performed where appropriate to measure statistical significance (GraphPad Prism 5.02, GraphPad Software). Differences were taken to be significant for $p < 0.05$.

3.3. Results and discussion

3.3.1. GGMA and GelMA synthesis

The mechanical properties of hydrogels mainly depend on the original rigidity of polymer chains and the crosslinking density [110]. GG, a polysaccharide, is composed of rigid repeat units that have six-membered ring structure, and have many hydroxyl groups that can be functionalized with the photoreactive methacrylate groups of which the amount determines the crosslink density of the resulting network. Thus, if GG is highly methacrylated, it can be a suitable candidate for the stiff first network of a DN hydrogel. In contrast, gelatin has a more flexible chain, and a relatively small amount of the amine groups of lysine or hydroxylysine residues are spread throughout the polymer. Consequently, methacrylated gelatin can be adequate for the soft and ductile second network. Molecular weight was also an important factor to be considered. As it was reported that the concentration of the second component must be much higher than the first component for the DN to effectively improve the mechanical properties [41], the first polymer had to form rigid hydrogels at low polymer concentration, which meant that the molecular weight of the first polymer had to be very high. Furthermore, the stiffness of a hydrogel increases as the molecular weight of the polymer increases, because the effective number of crosslinked chains increases [135]. Considering all these factors, GG with the molecular weight of ~1 MDa and gelatin were chosen as each the first and the second polymer for this study.

Both polymers were methacrylated by reacting them with methacrylic anhydride [20, 148] (Figure 3.1A-B). The DM of GGMA analyzed by using ^{1}H NMR spectroscopy was 24.5%. Since

one repeating unit has 10 hydroxyl groups, the DM of 24.5% means that there were 2.45 methacrylate groups per repeating unit, so the molecular weight between two methacrylate groups is about 300 g/mol on average. In case of gelatin, the DM was calculated to range from 5.7% to 76.0%, which was created by varying the amount of methacrylic anhydride added to the synthesis reaction to examine the effect of the crosslink density of the second network to the mechanical properties of DN hydrogels. Since the molecular weight of a gelatin molecule is around 100 kDa [154], the molecular weight between two metharylate groups in GelMA was calculated to range from 4,000 to 50,000 g/mol on average. Consequently, highly methacrylated gellan gum and methacrylated gelatin were successfully prepared as the first and the second component of DN hydrogels.

3.3.2. Fabrication of DN hydrogels

DN hydrogels were fabricated by a two-step crosslinking (Figure 3.1C). First, the GGMA solutions (0.5%, 1.0%, 1.5% (w/v)) were photocrosslinked to form the first network, GGMA hydrogels. The GGMA hydrogels then were immersed in GelMA solution (5%, 10%, 15%, 20% (w/v)) so that the GelMA molecules can diffuse into the GGMA hydrogels. Since the initial polymer concentration of the GGMA hydrogels was much lower than the concentration of GelMA solution, the hydrogels deswelled in GelMA solution likely due to the osmotic pressure. Subsequently, the gels were taken out and exposed to light for the second crosslinking. To confirm that the GelMA molecules diffused into the GGMA gels, 0.5% GGMA hydrogels were immersed in 20% GelMA (DM:14.7%) solution containing FITC-GelMA, and the fluorescence image of the gel cross-section was taken at each time point (Figure 3.2A-E). The relative fluorescence intensity profile in the middle of the cross-section at each time point was plotted to show that GelMA molecules diffused into the GGMA gel, and the concentration of GelMA molecules became almost uniform in the GGMA gel in several hours. We estimated the diffusion coefficient (D) of GelMA molecules in the GGMA hydrogel by using these plots. Assuming that the diffusivity is constant and the diffusion in this case can be seen as a one-dimensional diffusion, the diffusion equation has the solution [155, 156]

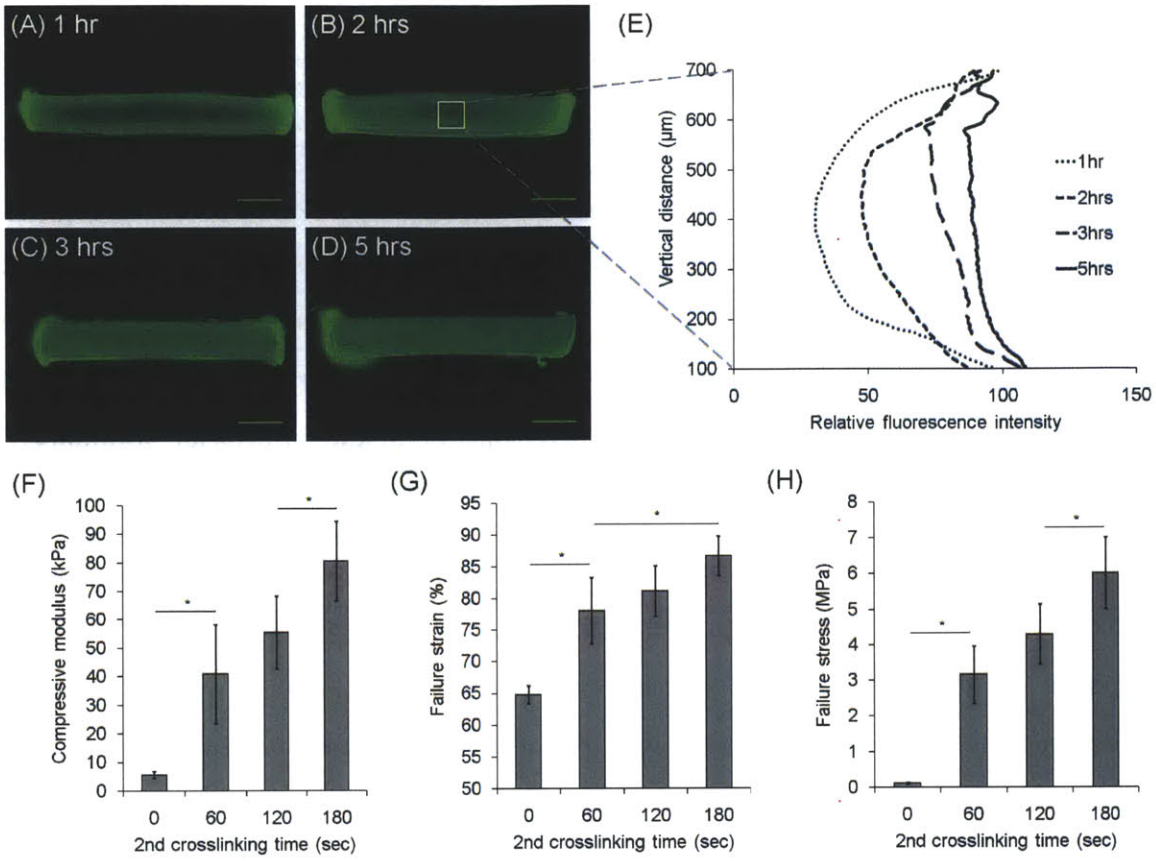

Figure 3.2. Formation of double-network (DN) hydrogels. (A-D) Diffusion of FITC-GelMA molecules into GGMA hydrogels over time. (A) 1hr, (B) 2hrs, (C) 3hrs, (D) 5hrs. Scale bars represent 1 mm. (E) Vertical fluorescence profile of the cross-section of hydrogels over time. (F) Compressive modulus, (G) failure strain, and (H) failure stress of DN hydrogels with varying 2nd crosslinking time. 0.5% GGMA hydrogels crosslinked for 120 seconds and 20% GelMA(DM: 14.7%) solutions were used for (A)-(H). (*) indicates significant difference ($P < 0.05$).

$$c(x,t) = c_0\left(1 - \frac{1}{2}\sum_{n=-\infty}^{\infty}\left\{\left[\mathrm{erf}\left(\frac{(2n+1)d-x}{2\sqrt{Dt}}\right) - \mathrm{erf}\left(\frac{2nd-x}{2\sqrt{Dt}}\right)\right] - \left[\mathrm{erf}\left(\frac{2nd-x}{2\sqrt{Dt}}\right) - \mathrm{erf}\left(\frac{(2n-1)d-x}{2\sqrt{Dt}}\right)\right]\right\}\right)$$

where c_0 is the initial concentration at boundaries, d is the thickness of the hydrogel, and erf is the error function. Although the thickness of the GGMA hydrogels decreased due to the deswelling in the GelMA solution, we used the final thickness of DN hydrogels for d, because most of the deswelling occurred within an hour, and the expected error was not significant in further estimation and comparison. By fitting the fluorescence profiles in the solution above retaining the terms with $n = 0, \pm 1$, and ± 2, D was estimated as (8 ± 3) x 10^{-8} cm^2/s. In the literature, the diffusion coefficient of gelatin in water was reported to be on the order of 10^{-7}

cm^2/s [157, 158]. The hydrodynamic radius of gelatin molecules can be estimated to be ~10 nm; the ratio of diffusion coefficients in water and in hydrogels of macromolecules of this size was reported to be around 0.5 for several studies [159, 160]. Therefore, the estimated value of D above is feasible. Using the calculated value of diffusivity, it was estimated that it would take ~6 hrs for the concentration of GelMA at the center of GGMA hydrogel with thickness of 800 μm to be 90% of that at the boundaries, ~7 hrs for 95%, and ~11 hrs for 99%. Using the equation above retaining more terms with higher n does not make significant difference. The effect of shaking is presumably to reduce the resistance to mass transfer in the interfacial boundary layer outside the gel.

Diffusion of GelMA molecules into GGMA hydrogels was also confirmed by the enhancement of the mechanical properties of the resulting gels. The immersed gels were taken out, exposed to light for the second crosslinking for varying times, and tested by compressions on a mechanical tester. Compared to the gels that were not exposed to light (0 s), the gels that were exposed to light presented enhanced mechanical properties, which confirms the formation of the second network (Figure 3.2F-H). The compressive modulus, failure stress, and failure strain of the gels all continued to increase with increasing crosslinking time up to 180 s, the maximum time that was tested. The formation of the second network might not be complete in 180 s, so further crosslinking may further enhance the mechanical properties. However, longer crosslinking times are potentially detrimental for cell encapsulation, so for further experiments the second crosslinking time was set at 120 s.

The interconnection between the two networks is an important factor that affects the mechanical properties of DN hydrogels. It was reported that DN hydrogels with no interconnection between the two networks can be stronger than those with the interconnection because the interconnection sites serve as the crosslinking sites of the second network, so if there are too many interconnections, the second network would not be crosslinked loosely enough [161]. Since both GGMA and GelMA networks are formed via the same mechanism, the unreacted C=C double bonds of the metheacrylate groups in the GGMA network can react during the GelMA network formation. To examine the amount of the unreacted double bonds in GGMA hydrogels, FTIR spectra were taken for GGMA hydrogels with

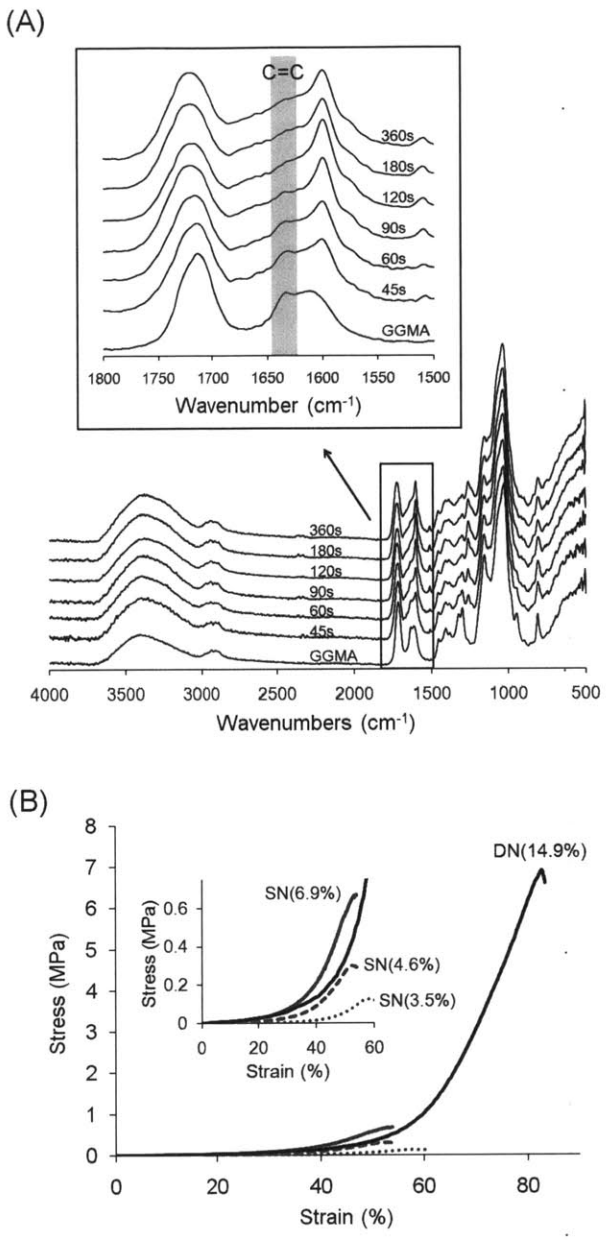

Figure 3.3. (A) FTIR spectra of GGMA and dried GGMA hydrogels crosslinked for varying time. The shoulder peak appearing around 1640cm^{-1} corresponds to the unreacted C=C bonds. (B) Stress-strain curves of GGMA/GelMA SN and DN hydrogels with the same mass ratio (GelMA/GGMA = 8.2). Every crosslinking time was 120 seconds, and GelMA (DM: 32.3%) was used. The number in parenthesis refers to the polymer content of the hydrogels.

varying crosslinking time (Figure 3.3A). It was found that the shoulder peak appearing around 1640cm^{-1} corresponding to the unreacted C=C double bonds decreased over crosslinking time and almost disappeared in 120s, which meant most of the C=C double bonds reacted. Further

crosslinking up to 360s did not significantly change the spectrum. Although this is a qualitative result and there may be a small fraction of unreacted double bonds, the crosslinking time was kept at 120s for further experiments since shorter crosslinking time is better for cell viability. Even though there may be a small amount of interconnection, the resulting DN hydrogels (prepared from 0.5% GGMA hydrogels immersed in 20% GelMA solution) were significantly stronger than the GGMA/GelMA SN hydrogels with the same mass ratio (GelMA/GGMA = 8.2, this will be discussed later in Figure 3.6) prepared by a single crosslinking of GGMA/GelMA mixed solutions (Figure 3.3B). It was found that GGMA/GelMA SN hydrogels with the polymer content as high as that of DN hydrogels (14.9%) could not be prepared since it was not possible to dissolve both polymers together at such a high concentration. The GGMA/GelMA SN hydrogels with lower polymer content failed at much lower strain and stress, which indicates that they are more brittle and weaker than DN hydrogels. Based on Figure 3.3B, it is expected that even if we made the SN hydrogels with the same polymer content, they would fail at lower strain and stress than DN hydrogels.

3.3.3. Mechanical properties of DN hydrogels

The mechanical properties of DN hydrogels were measured by unconfined, uniaxial compression tests on a mechanical tester, and compared with those of GGMA and GelMA SN hydrogels (Figure 3.4). The modulus of DN hydrogels made from 0.5% GGMA hydrogels immersed in 20% GelMA (DM: 32.3%) solution was significantly higher than that of SN hydrogels. It may seem strange that the modulus of GGMA hydrogel is lower than that of GelMA hydrogel as the first network must be stiffer than the second network, and that the modulus of DN hydrogel became very high by combining two networks with relatively low modulus. In order to explain this, it should be considered that these mechanical data were obtained from swollen hydrogels, and the modulus of a hydrogel greatly depends on the polymer content in the swollen state. Even though the GGMA hydrogel barely swelled in water, since it was formed at very low concentration (0.5%), the polymer content of the swollen GGMA hydrogel was only 0.46 ± 0.05 %, while the 20% GelMA hydrogel swelled to a much higher degree, but still had a high polymer content, 9.5 ± 0.2 %. Considering that the modulus

of 1.0% GGMA hydrogel with the polymer content of 1.1 ± 0.1% had a similar modulus to that of GelMA20% (data not shown), it is true that GGMA network is stiffer than GelMA network. Also, GGMA hydrogels were brittle, breaking at less than 40% of strain, while GelMA hydrogels did not break up to 80% of strain. The polymer content of the resulting DN hydrogel was even higher, 14.9 ± 0.6 %. This is likely because the swelling of the GelMA network was restricted since it was formed in the GGMA network. In addition, as mentioned earlier, the GGMA hydrogels deswelled in GelMA solution likely due to the osmotic pressure, and the final volume of the DN gels in the swollen state was smaller than that of the initial GGMA hydrogels. Thus, the increased concentration of GGMA in DN hydrogels was also the reason for the high polymer content. Along with the effect of DN, this higher polymer content also caused the DN hydrogels to have much higher modulus.

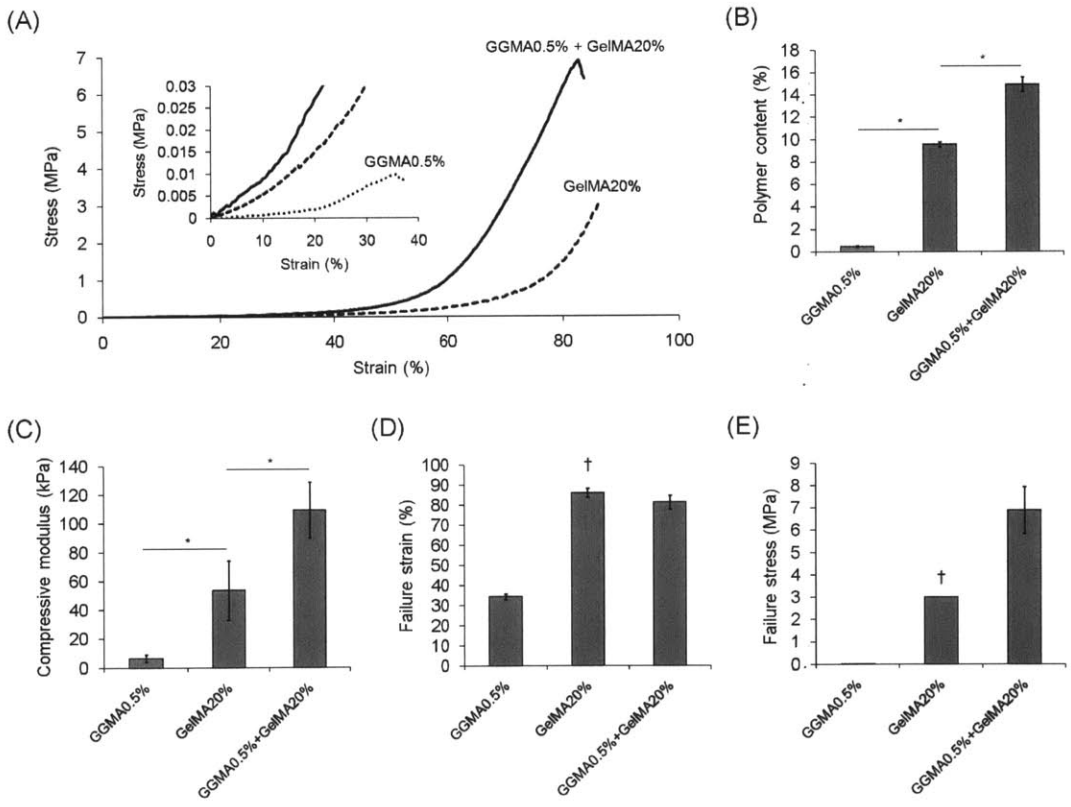

Figure 3.4. (A) Stress-strain curves for SN and DN hydrogels under uniaxial compression. (B) Polymer content, (C) compressive modulus, (D) failure strain, and (E) failure stress of SN and DN hydrogels. (†) indicates the stress under which the majority of GelMA SN gels started to break, and the strain at that stress. Every crosslinking time was 120 seconds, and GelMA (DM: 32.3%) was used for (A)-(E). (*) indicates significant difference ($P < 0.05$).

We found that GelMA (DM: 32.3%) SN hydrogels were quite strong by themselves, such that the failure stress reached up to a few MPa (80% of hydrogels tested broke under 3 MPa, while 20% broke under 2.5 MPa), which is not usually observed for SN hydrogels. The DN hydrogels exhibited even higher failure stress than SN hydrogels, 6.9 ± 1.0 MPa. This higher strength of the DN hydrogels results from a combination of an increase in the equilibrium polymer concentration and the DN structure. DN formation enabled higher polymer content in the swollen state without increasing the crosslink density as is required to increase concentration for SN hydrogels, which leads to brittle gels. Thus, along with the crack energy dissipation to the second network, the higher polymer content of these DN hydrogels without the increase of crosslink density is a great advantage that enables them to resist higher stress. To confirm that DN hydrogels are stronger than SN hydrogels even when their polymer contents are similar, GelMA SN hydrogels with polymer content of 15.3 ± 0.3 % were made from a 15% solution of GelMA with higher DM (65.2%). It was found that 80% of these DN hydrogels tested broke under 2 MPa, which shows that they were weaker than DN hydrogels with similar polymer content, and even weaker than GelMA (DM: 32.3%) SN hydrogels with a lower polymer content.

To examine the effect of the crosslink density of the GelMA network on the mechanical properties of DN hydrogels, GelMA polymers with varying DM were synthesized and used to make DN hydrogels (Figure 3.5). The DM of GelMA increased up to ~30% almost linearly with the amount of metharcrylic anhydride added to the reaction, but over ~30%, the conversion increased more slowly with increasing methacrylic anhydride concentration. The compressive modulus of DN hydrogels increased as the DM of GelMA increased due to the increase in crosslink density of the second network and the polymer content of DN hydrogels. Since the GelMA polymer with higher DM is more hydrophobic, the DN hydrogels resulting from it swelled less in water and presented higher polymer content in swollen state. However, the failure strain and the failure stress had a maximal value, 81 ± 3 % and 6.9 ± 1.0 MPa at the DM of 32.3%. This demonstrates that a certain amount of crosslink is needed to make substantial gel that can work effectively as the second network, but if the second network gets crosslinked too much, it becomes brittle and its capacity of energy dissipation decreases. The intermediate

crosslink density that shows maximal failure stress optimizes the trade-off between stiffness and the strength of the DN hydrogels.

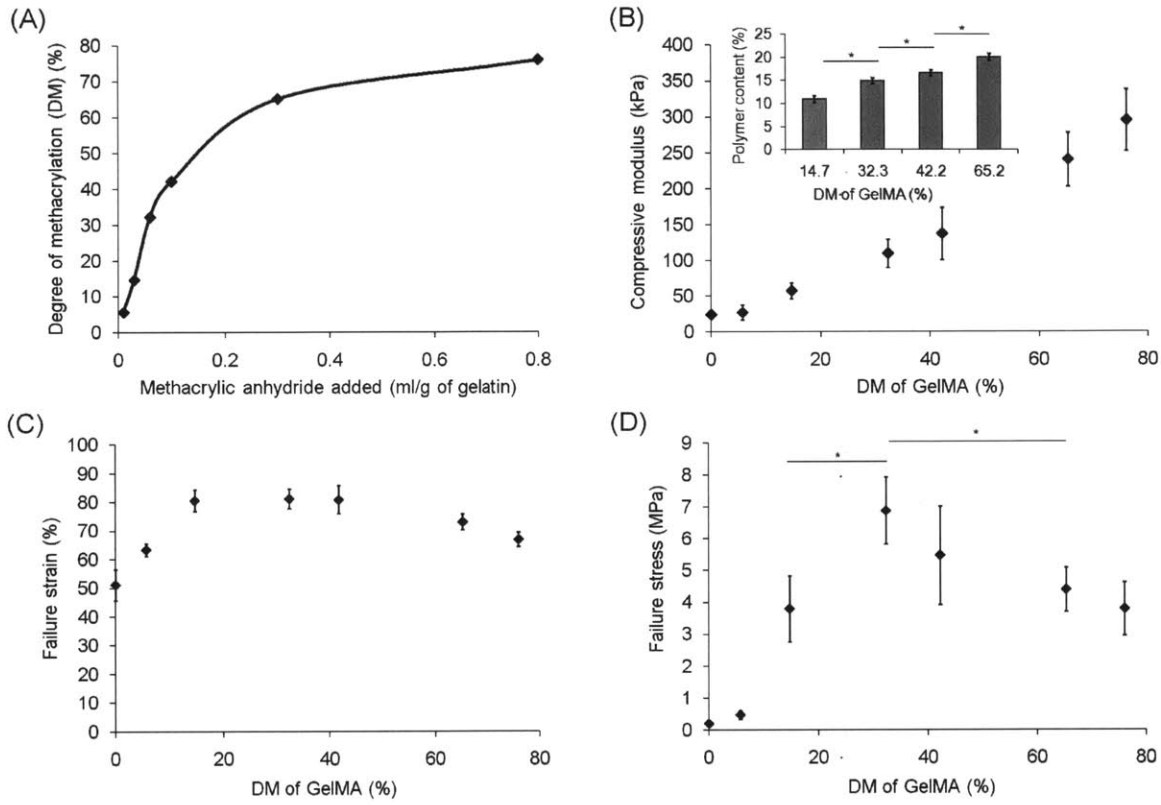

Figure 3.5. (A) Degree of methacrylation (DM) of GelMA with varying amount of methacrylic anhydride added to the reaction. (Inset in B) Polymer content of DN hydrogels with varying DM of GelMA. Effect of DM of GelMA on (B) compressive modulus, (C) failure strain, and (D) failure stress of DN hydrogels. Every crosslinking time was 120 seconds. 0.5% GGMA hydrogels and 20% GelMA(each DM) solutions were used for (A)-(E). (*) indicates significant difference ($P < 0.05$).

The concentration of each component in the preparation of DN hydrogels also had great influence on the mechanical properties (Figure 3.6). When the concentration of the first GGMA hydrogels varied from 0.5% to 1.5%, while that of GelMA (DM: 32.3%) solution was kept at 20%, the mass ratio of GelMA to GGMA in the resulting DN hydrogels decreased from 8.2 to 6.2. The reason for that the mass ratio decreased by only 24% of the initial value while the concentration of GGMA was tripled is that the higher the GGMA concentration, the less the GGMA hydrogels deswelled in GelMA solution. Due to the stiffness of the GGMA network, the

modulus of the DN hydrogels significantly increased as the GGMA concentration increased. However, the failure strain and stress dropped greatly. This indicates that the mass ratio of the second to the first network must be very high to get strong DN hydrogels, consistent with previous results [41, 47]. When the concentration of GelMA solution was varied from 5% to 20% while the GGMA concentration was kept at 0.5%, the compressive modulus did not vary significantly. However, increasing the concentration of GelMA increased the mass ratio from 5.2 to 8.2, resulting in significant increases in the failure strain and stress. Achieving a high mass ratio of the second to the first network was an important reason for choosing the GGMA with a high molecular weight as the first component since polymers with high molecular weights can form hydrogels at very low concentrations. It was difficult to prepare DN hydrogels with even higher mass ratios because GGMA polymer could not form hydrogels at lower concentrations than 0.5%, and GelMA solutions with higher concentration than 20% were too viscous to process. However, increasing the molecular weight of GG may allow gelation at a lower concentration, enabling stronger DN hydrogels by further increasing the mass ratio of the second network to the first network.

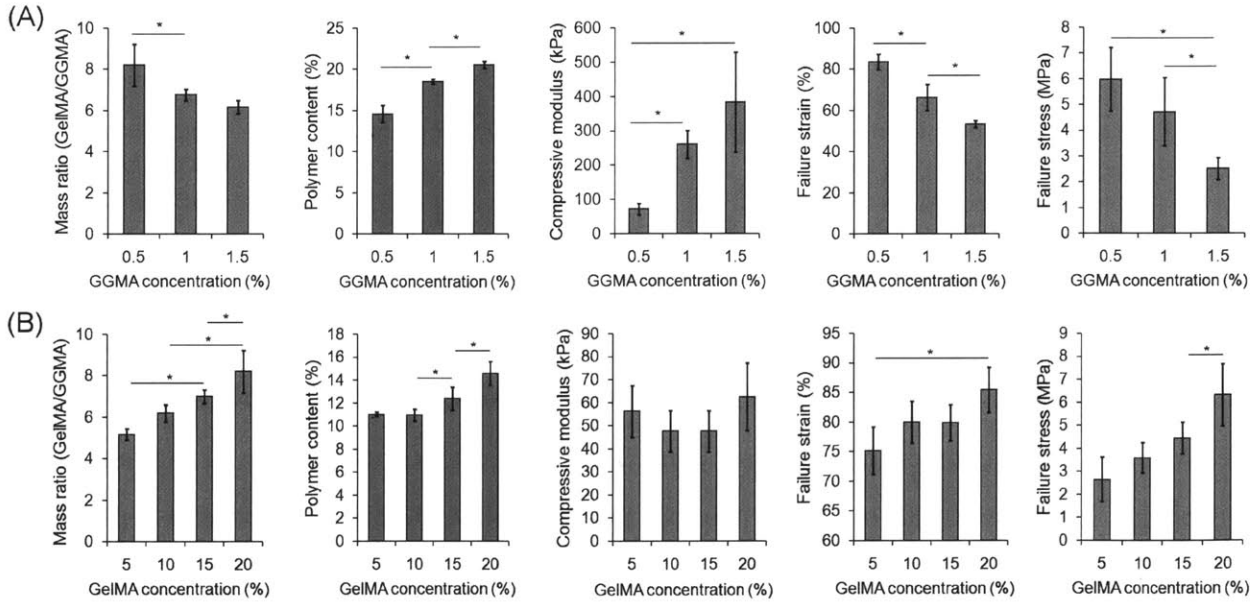

Figure 3.6. Mass ratio (GelMA/GGMA), polymer content, compressive modulus, failure strain, and failure stress of DN hydrogels with varying concentration of either component: (A) varying concentration of GGMA hydrogels + 20% GelMA solution, and (B) 0.5% GGMA hydrogels + varying concentration of GelMA solution. GelMA (DM: 32.3%) was used for (A)-(B). (*) indicates significant difference ($P < 0.05$).

3.3.4. Encapsulation of cells in DN hydrogels

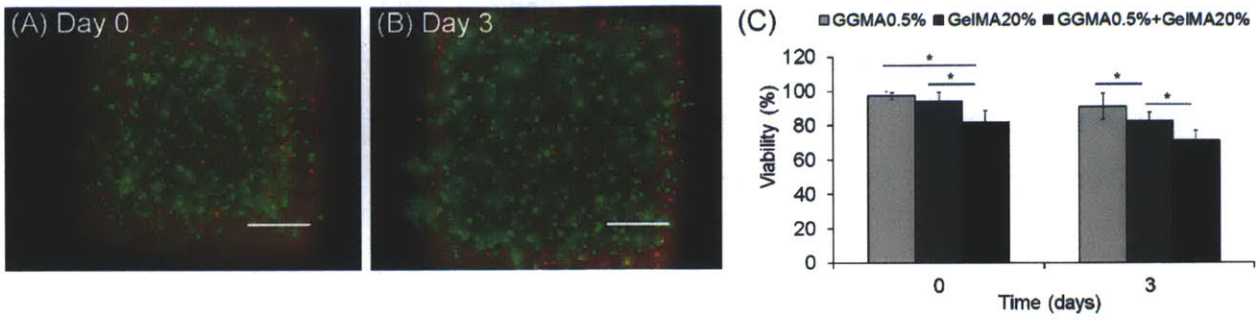

Figure 3.7. Fluorescence images of live/dead stained NIH-3T3 fibroblasts encapsulated in DN hydrogels: (A) day 0 and (B) day 3 of culture after DN hydrogel formation. Scale bars represent 200μm. (C) Viability of 3T3 fibroblasts encapsulated in SN and DN hydrogels. (*) indicates significant difference ($P < 0.05$). 0.5% GGMA hydrogels and 20% GelMA (DM: 14.7%) solutions were used for (A)-(C).

To fabricate cell-laden tissue constructs for tissue engineering applications, cells encapsulated in the DN hydrogels must survive the entire DN synthesis process. To make cell-laden DN hydrogels, we encapsulated cells in the first network, GGMA hydrogels, by crosslinking the mixture of cell suspension and GGMA solution. Subsequently, the cell-laden GGMA hydrogels were immersed in GelMA solution containing the photoinitiator, followed by the second crosslinking. The cell viability of encapsulated NIH-3T3 fibroblasts in the DN hydrogels was measured at two time points, day 0 and day 3 (Figure 3.7). The cell viability tested by using live/dead staining 1 hour after the DN formation (Day 0) was 82%, and after 3 days of culture, the cell viability was measured to be 71%. Although the cell viability in DN hydrogels was lower than that in each GGMA and GelMA SN hydrogels, it is as good as in some previous reports on the cell viability in photocrosslinked hyrogels [13, 20, 128]. This result demonstrates that the majority of cells survived the whole DN formation process, that is, the two crosslinking steps under light and the immersion step between them in a viscous solution containing the photoinitiator. As shown in Figure 3.2, longer crosslinking time may enhance the mechanical properties of the DN hydrogels; however, it is likely to result in a lower cell viability. Immersion in the viscous solution with the photoinitiator may also harm the cells, thus making the immersion time shorter would increase the cell viability. However, shortening the

immersion time will limit the size of the DN constructs since time is required to allow the second polymer to diffuse in the first network. Thus, encapsulating cells in this DN system can be further optimized by controlling the crosslinking conditions and immersion time that closely relates to the cell viability, the size of the constructs, and the mechanical properties. Further cell experiments such as a tissue formation in DN hydrogels and the resulting change in mechanical properties over time will be performed in the future.

3.4. Conclusion

In this study we developed mechanically strong DN hydrogels that can encapsulate cells for applications as scaffolds for load-bearing tissues. Cell-laden DN formation was made possible by using a two-step photocrosslinking of two modified biomacromolecules, GGMA and GelMA, which are photoreactive versions of gellan gum and gelatin. As compared to SN hydrogels, DN hydrogels exhibited higher strength, which approaches closer to the strength of cartilage. It was found that a certain range of DM of the second network is optimal to achieve highest strength of the DN hydrogels, and a large mass ratio of the second to the first network is needed to obtain strong DN hydrogels. The encapsulation of NIH-3T3 fibroblasts and the following cell viability assay presented that the whole DN formation process was cell-compatible. Given the high mechanical strength and the cell-compatibility, our DN hydrogels made from photocrosslinkable macromolecules have great potential in applications as scaffolds for the load-bearing tissues.

Chapter 4: Gellan gum microgel-reinforced cell-laden gelatin hydrogels

The content of this chapter has been accepted in the following journal article: Shin H, Olsen BD, Khademhosseini A. Gellan gum microgel-reinforced cell-laden gelatin hydrogels. Journal of Materials Chemistry B, DOI: 10.1039/C3TB20984A.

4.1. Introduction

Natural tissues have various mechanical properties according to their functions. Tissues such as cartilage, tendon, and bone have great strength because they have to sustain large loads every day. Tissue engineering scaffolds for such load-bearing tissues must therefore have high strength to keep their integrity after being implanted to the load-bearing positions. In this regard, the mechanical weakness of most hydrogels is a major limitation, although they have been considered as a promising candidate for tissue scaffolds due to their advantages such as high water content, permeability, biocompatibility, and ability to encapsulate cells in a three-dimensional environment.[8, 9, 162] Several new platform materials have been developed to improve the mechanical strength of hydrogels, such as double-network (DN) hydrogels[47, 49, 147], polyrotaxane hydrogels[43], nanocomposite hydrogels[44], ideally homogeneous tetra-PEG hydrogels[42], ionically cross-linked triblock copolymer hydrogels[45], and shear thinning protein hydrogels reinforced by block copolymer self-assembly[46].

Previously we developed cell-laden DN hydrogels by using a cell-compatible two-step photocrosslinking method.[163] Photocrosslinkable gellan gum (GG) was used to make the stiff first network, and photocrosslinkable gelatin was used to make the soft and ductile second network. The strengthening mechanism of DN hydrogels was elucidated that the first network works as a stiff scaffold that sustains the stress throughout the construct, and the soft and ductile second network dissipates the crack energy preventing the failure of the construct.[51] We adapted this strategy for making cell-laden hydrogels from two photocrosslinkable biomacromolecules. The resulting DN hydrogels exhibited significantly higher strength than single network hydrogels, and the cells were highly viable after encapsulation in DN hydrogels. Further research into the materials as tissue engineering scaffolds determined that these DN

hydrogels weakened when they were prepared in cell-compatible solutions, and the encapsulated cells did not function as well as in gelatin alone.

Motivated by the need to develop better hydrogel system in terms of both mechanical strength and biological properties, we decided to use the microgel-reinforced (MR) hydrogel strategy with the same materials that were used to make the DN hydrogels. MR hydrogels were previously fabricated by embedding stiff microgels into a soft and ductile matrix.[56, 164] The MR hydrogels exhibited significantly higher strength than the hydrogels with no microgels, and comparable strength to DN hydrogels. The simple difference between MR and DN hydrogels is that the stiff hydrogel is incorporated into the soft and ductile hydrogel as microparticles in MR hydrogels, not as bulk hydrogel as in DN hydrogels. By this difference, we expected two advantages of our MR hydrogels for our purpose. First, although the GG component had to be prepared at relatively low polymer concentrations for DN hydrogels due to the adverse effect of GG/Gelatin mass ratio on the strength of DN hydrogels, for MR hydrogels, GG hydrogels prepared at higher polymer concentration can potentially increase the strength due to their higher stiffness. Second, because cells were encapsulated not in GG but in gelatin, the cells were expected to function better in MR hydrogels than in DN hydrogels.

In this study, we first prepared GG microgels using a water-in-oil emulsion followed by a light-initiated crosslinking. MR hydrogels were prepared by embedding the GG microgels into gelatin hydrogels and their mechanical properties were examined to compare with those of the DN hydrogels and the gelatin hydrogels with no microgels. MC3T3-E1 preosteoblasts were encapsulated in the MR hydrogels to examine their activity and osteogenic behavior by determining viability, metabolic activity, alkaline phosphatase (ALP) activity, and mineralization. Comparison with DN hydrogels from the same two polymers with the MR hydrogels indicates that the MR hydrogels have better biological performance, and may be of benefit as tissue scaffolds.

4.2. Materials and methods

4.2.1. Modification of GG and gelatin

GG (Gelzan^{TM}, MW: 1,000,000), gelatin (from porcine skin, Type A), and methacrylic anhydride were purchased from Sigma-Aldrich. Photocrosslinkable GG was prepared by reacting GG with methacrylic anhydride.[38] 3g of GG was dissolved in distilled water at 90°C and the solution was cooled down to 50°C. 24ml of methacrylic anhydride was added to the solution and the reaction was allowed to proceed for 4hrs at 50°C while the pH of the solution was adjusted to 8 by adding 15N NaOH. Then the reaction mixture was dialyzed in distilled water using dialysis membrane (MW cutoff: 12-14kDa, Spectrum Labs, Inc.) at 4°C for 6 days. The solution was frozen and lyophilized to obtain photocrosslinkable GG. The resulting material was kept at -40°C until further use. Similarly, photocrosslinkable gelatin was prepared by reacting gelatin with methacrylic anhydride.[20] 30g of gelatin was dissolved in 300ml of phosphate buffered saline (PBS, 1X, Life Technologies) at 50°C. 3ml of methacrylic anhydride was added to the solution and the reaction was allowed to proceed for 2hrs at 50°C. The reaction mixture was diluted with an equal amount of distilled water and dialyzed in distilled water at 40°C for 6 days. The resulting solution was lyophilized to obtain photocrosslinkable gelatin, and it was kept at -40°C until further use.

4.2.2. Preparation and characterization of microgels

GG microgels were prepared by using a water-in-oil emulsion.[165] Photocrosslinkable GG was dissolved in ultrapure water containing 1% (w/v) photoinitiator, 2-hydroxy-1-[4-(2-hydroxyethoxy) phenyl]-2-methyl-1-propanone (Irgacure 2959, BASF) at ~40°C to make solutions with varying GG concentrations (1.0%, 1.5%, 2.0%, 2.5%, (w/v)). 0.4ml of the GG solution was mixed with 5ml of mineral oil (Sigma-Aldrich) containing 0.02ml of Span 80 (Sigma-Aldrich), and the mixture was homogenized for 3mins by using an OMNI GLH homogenizer (OMNI International). The resulting emulsion was exposed to light (325-500nm, ~7.5mW/cm^2, EXFO OmniCure S2000) for 120s to obtain crosslinked GG microgels. The resulting solution was dried overnight at ~40°C with constant stirring to evaporate the water. GG microgels were separated from mineral oil by centrifugation at 5,000rpm, and washed with isopropanol,

hexane, and acetone, before they were dried under vacuum at room temperature for 3 days. The GG microgels were coded as GG1.0, GG1.5, GG2.0, and GG2.5 according to the polymer concentration in the GG microgels.

Scanning electron microscope (SEM) images of dried GG microgels were taken by using a JEOL JSM 6060 SEM with a 2.5kV accelerating voltage at a 10mm working distance. To prepare specimens, GG microgels were attached onto specimen stubs and sputter coated with gold/palladium (SC7640, Polaron).

Optical microscope images of microgels in PBS were taken by using an optical microscope (Zeiss AxioObserver. D1). The size of microgels in the images was measured by using the ImageJ software.

To measure the swelling ratio, GG microgels were allowed to swell in distilled water for 1hr to reach equilibrium in a tube with known weight. After centrifugation at 5,000rpm, the excessive water was removed and the weight of the wet microgels (W_s) was determined. The microgels were lyophilized and the dry weight (W_d) was determined. The swelling ratio was calculated as W_s/W_d.

4.2.3. Preparation and characterization of MR and DN hydrogels

GG microgels were allowed to swell in PBS containing 0.05% (w/v) photoinitiator to make solutions with varying GG concentrations (0.25%, 0.5%, 0.75%, 1.0% (w/v)). Photocrosslinkable gelatin was dissolved in these solutions to make 10% (w/v) gelatin solutions with GG microgels. The resulting mixtures were molded into disks with ~8mm diameter and ~1mm thickness, and exposed to light (~7mW/cm^2) for 180s. The resulting MR hydrogels were immersed in PBS and incubated at 37°C until further experiments. The MR hydrogels were coded as MRx-y, where x is the polymer concentration in the GG microgels, and y is the GG concentration in the MR hydrogels.

DN hydrogels were prepared with only minor modifications from the previously described method.[163] In short, photocrosslinkable GG was dissolved in distilled water containing 0.05% (w/v) photoinitiator at 0.5% (w/v), and the solution was crosslinked with the same method as above. The resulting GG hydrogels were immersed in photocrosslinkable gelatin

solution (10% (w/v) in PBS) containing 0.05% (w/v) photoinitiator at 37°C for 1 day. Subsequently, the hydrogels were taken out and the excess gelatin solution was removed from the surface of the hydrogels before they were exposed to light again for 180s. The resulting DN hydrogels were immersed in PBS at 37°C until further experiments.

The polymer concentration of MR hydrogels was determined as W_d/W_s where W_d is the weight of the dried MR hydrogels and W_s is the weight of the swollen MR hydrogels in distilled water. Before W_s was measured, the MR hydrogels were washed with distilled water three times to remove the salts in PBS.

The mechanical properties of hydrogels were determined by unconfined, uniaxial compression tests by using an Instron 5943 mechanical tester. The compression rate was $0.5mm/min^{-1}$. The compressive modulus was determined as the slope of the stress-strain curve in the 0-10% strain range. The failure stress was determined as the stress at which the slope of the stress-strain curve started to decrease where the hydrogels started to break.

To observe the microstructure of the hydrogels, SEM images of the cross-section of the hydrogels were taken by using a JEOL JSM 6060 SEM with a 5kV accelerating voltage at a 10mm working distance. To minimize changes to the hydrogel structure, the hydrogels were frozen very quickly by liquid nitrogen.[166] After being lyophilized, the cross-section of the hydrogels was attached onto specimen stubs and sputter coated with gold/palladium (SC7640, Polaron).

4.2.4. Cell culture and encapsulation

MC3T3-E1 cells were cultured using the growth media, which is Minimum Essential Medium Alpha (MEM Alpha, Life Technologies) supplemented with 10% fetal bovine serum (FBS, Life Technologies) and 1% penicillin-streptomycin (Life Technologies) in 5% CO_2 in air atmosphere at 37°C. Media was replaced every 2-3 days and cells were passaged every 3-4 days when they are 70-80% confluent on the culture flasks.

Photocrosslinkable gelatin solutions (10% (w/v)) with 0.5% and 1.0% of GG1.5 microgels were prepared in PBS containing 0.05% (w/v) photoinitiator at 37°C. Cells were trypsinized and resuspended into these solutions to make $5x10^6$ cells/ml suspensions. The suspensions were pipetted on a Petri dish between two spacers with 600μm thickness and covered with a glass

slide. Subsequently they were exposed to light (~7mW/cm^2) for 180s to obtain cell-laden MR hydrogels. Similarly, a photocrosslinkable GG solution (1.5% (w/v)) was prepared in PBS containing 0.05% photoinitiator at 37°C, and cell-laden GG hydrogels were prepared with the same method as above. The resulting GG hydrogels were immersed in a photocrosslinkable gelatin solution (10% (w/v) in culture media containing 0.05% photoinitiator) at 37°C for 1day. Then the hydrogels were taken out and the excess gelatin solution was removed from the surface of the hydrogels. The hydrogels were exposed to light (~7mW/cm^2) again for 180s to obtain cell-laden DN hydrogels. The resulting cell-laden MR and DN hydrogels were cultured in 5% CO^2 in air atmosphere at 37°C in the differentiation media, which is the growth media supplemented with L-ascorbic acid 2-phosphate sesquimagnesium (50μg/ml) and β-glycerophosphate disodium (10mM)[167]. The media was replaced every 2-3 days.

4.2.5. Cell behavior analysis

The cell viability was examined by using a LIVE/DEAD Viability Kit (Life Technologies) according to the manufacturer's instruction. The cell-laden hydrogels stained with calcein AM/ethidium homodimer-1 were visualized with a Nikon Eclipse Ti fluorescence microscope (Nikon), and the cell viability was determined as the number of live cells over the number of all cells.

The metabolic activity was examined by AlamarBlue (Life Technologies) assay. The cell-laden hydrogels were incubated with 300μm AlamarBlue reagent solution (10% (v/v) in growth media) at 37°C for 4hrs. Then the fluorescence (544Ex/590Em) of the solution was measured by using a FLUOstar plate reader (BMG). The reduction of the reagent was calculated as $(F_S-F_B)/(F_S-F_F)$ where F_S is the fluorescence of the sample, F_B is that of the untreated reagent solution, and F_F is that of the 100% reduced solution which was prepared by autoclaving the reagent solution.

ALP activity was measured by using an ALP assay kit (Abcam). The cell-laden hydrogels were disrupted by using a TissueLyser (Qiagen) before 5mM *p*-nitrophenyl phosphate (*p*NPP) solution in the assay buffer was added to the disrupted sample. After incubation for 6hrs at room temperature, the absorbance was measured at 405nm. In order to normalize the ALP activity by the amount of DNA, the DNA was quantified by using a PicoGreen dsDNA Assay Kit

(Life Technologies). The disrupted samples were incubated at room temperature for 5mins with the PicoGreen reagent solution in TE buffer before the fluorescence (485Ex/520Em) was measured.

Mineralization was examined by using Alizarin Red S (Sigma-Alrich) according to an Osteogenesis Assay Kit instruction (Millipore). The cell-laden hydrogels were fixed with 4% paraformaldehyde for 30mins, and stained for 5mins with 2% Alizarin Red S solution of which the pH was adjusted to ~4.2 by using 10% acetic acid. Then the hydrogels were washed with distilled water several times to remove all unreacted reagents. The images of the stained samples were taken by using a zoom microscope (Axio Zoom. V16, Zeiss). The samples were then left overnight with 10% acetic acid, heated to 85°C for 10 mins, and neutralized to pH of 4.1-4.5 with 10% ammonium hydroxide. Finally the absorbance was measured at 405nm.

4.2.6. Statistics

All data were expressed as mean ± standard deviation. The data were analyzed by using one-way or two-way ANOVA and Bonferroni test to determine statistical significance (GraphPad Prism 5.02, GraphPad Software). Differences were taken to be significant for $p<0.05$.

4.3. Results and discussion

4.3.1. Preparation and characterization of microgels

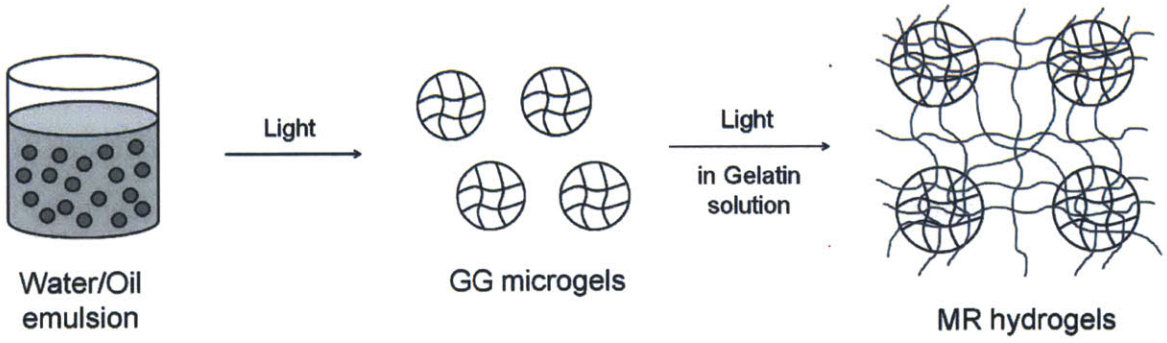

Figure 4.1. Preparation procedure of MR hydrogels.

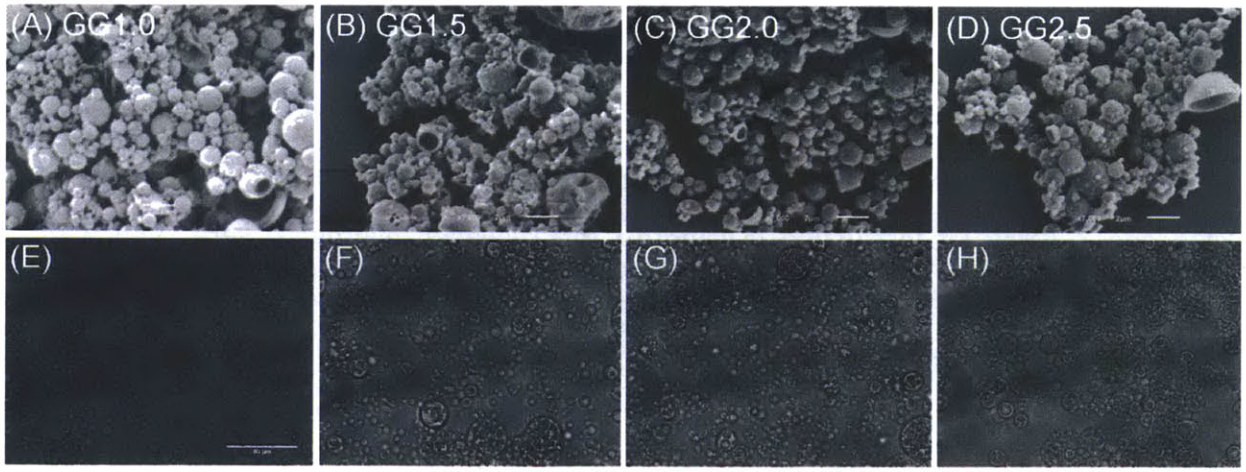

(I)

	Size (μm)
GG1.0	7.1±4.1
GG1.5	5.7±2.1
GG2.0	6.2±2.9
GG2.5	7.7±3.4

(J)

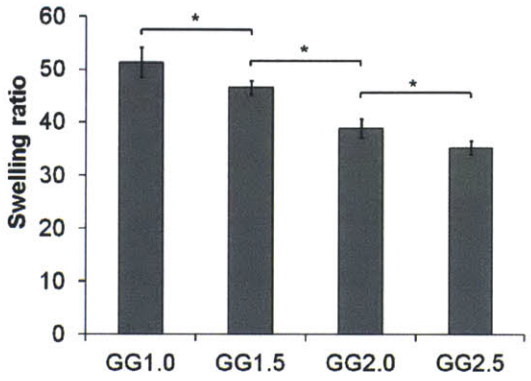

Figure 4.2. SEM (A-D) and optical microscope images (E-H) of GG microgels prepared at different polymer concentrations: (A,E) GG1.0, (B,F) GG1.5, (C,G) GG2.0 (D,H) GG2.5. The scale bars in (A-D) represent 2μm, and the scale bar in (E) represents 50μm. (I) Particle size of GG microgels in PBS. (J) Swelling ratio of GG microgels in distilled water. (*) indicates significant difference ($p<0.05$).

GG molecules consist of rigid repeat units that have many hydroxyl groups available for functionalization with photoreactive methacrylate groups.[38] Thus, hydrogels prepared by photocrosslinking highly methacrylated GG are relatively stiff with the moduli that are >100kPa at the polymer concentrations of only a few percentile, which make them a potentially useful reinforcement material. GG particles were prepared at four different concentrations (1.0%, 1.5%, 2.0%, 2.5%) by using water-in-oil emulsion followed by a light-initiated photocrosslinking (Figure 4.1). Since the emulsion was not transparent, a high concentration of the photoinitiator (1.0%) was used for the crosslinking. The SEM images of the GG microgels (Figure 4.2. (A-D))

showed that the resulting microgels were polydisperse and the size of the dried microgels ranged from a few micrometers to hundreds of nanometers. In PBS, the GG microgels swelled and the mean size of particles was measured to be several micrometers (Figure 4.2. (E-I)). The standard deviation of the size was large due to the high polydispersity of the microgels. No significant difference in the microgel size was observed with increasing the polymer concentration in GG microgels. This is probably because the viscosity of the aqueous GG solution was not high enough to affect the emulsion-forming process, and the GG microgels were highly crosslinked such that their swelling in PBS did not depend strongly on the GG concentration. The swelling ratio of the GG microgels (Figure 4.2. (J)) decreased as GG concentration increased, which is reasonable because the swollen size in a solution is similar while the polymer concentration increases with GG concentration.

4.3.2. Preparation and characterization of MR hydrogels

Loosely crosslinked gelatin hydrogels are soft and ductile, with the modulus of a few tens of kPa at 10% polymer concentration. Various amounts of the GG microgels were added to 10% photocrosslinkable gelatin solutions in PBS before the mixture was photocrosslinked to obtain MR hydrogels (Figure 4.1). The polymer concentration (w/w) of the MR hydrogels increased as the GG concentration in MR hydrogels increased, but no significant difference was observed among different GG concentrations of the microgels (Figure 4.3. (A)). Although the microgels can serve as additional crosslinks that constrain gelatin molecules from swelling,[57] thus microgels with different concentrations might have led to different polymer concentrations, the gelatin hydrogels were sufficiently crosslinked that they did not swell appreiciably in water, which is presumed to be the reason that microgel formulation did not affect the polymer concentration of the MR hydrogels. It is presumed that the reason that the polymer concentration increased by ~3% with only 1% of GG concentration added in MR hydrogel is that the lower hydrophilicity of GG molecules due to the high degree of methacrylation resulted in the lower water content in the wet state.

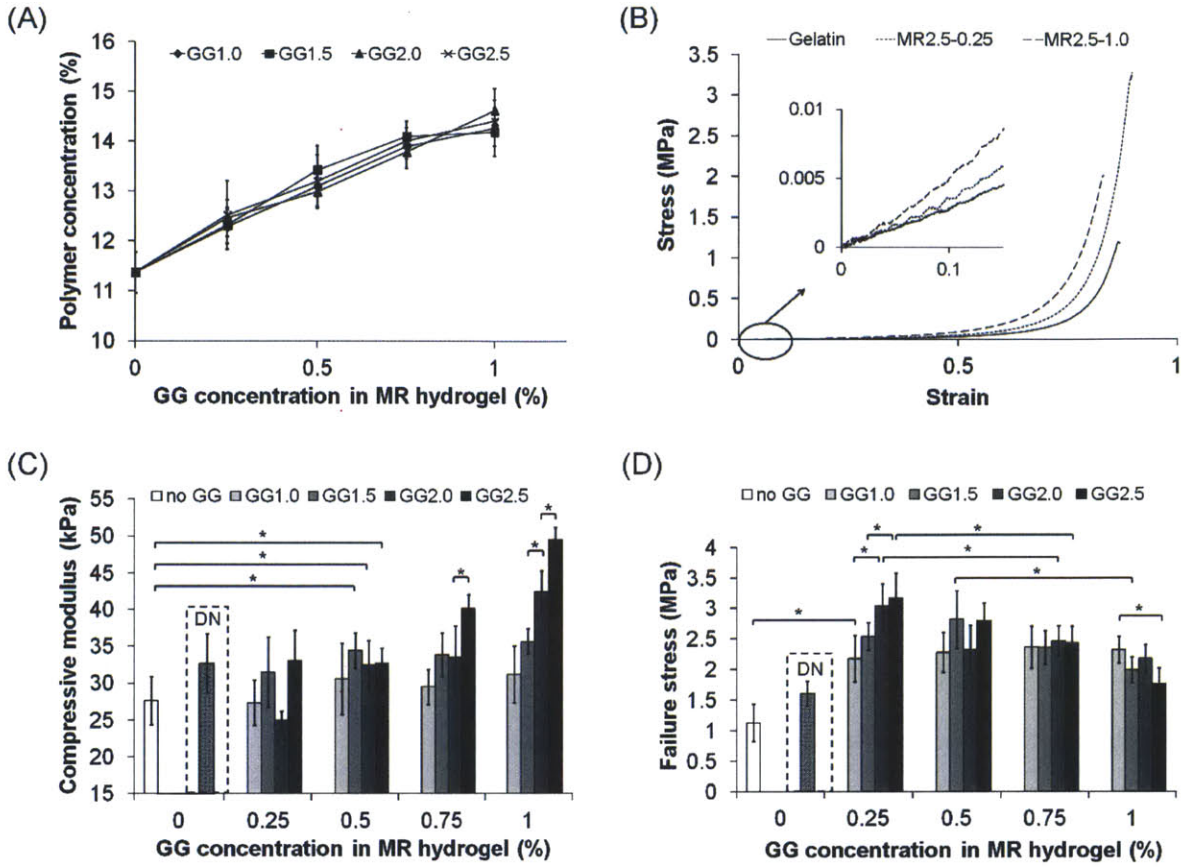

Figure 4.3. Polymer concentration of MR hydrogels (A) and mechanical properties of gelatin and MR hydrogels: (B) stress-strain curve (MRx-y: GG concentration is x% in microgels and y% in MR hydrogels), (C) compressive modulus and (D) failure strength. Compressive modulus and failure stress of DN hydrogels are added for comparison in (C) and (D) in each dotted box. (*) indicates significant difference ($p<0.05$).

The mechanical properties of MR hydrogels were determined by unconfined, uniaxial compression tests. Figure 4.3. (B) compares the stress-strain curves of two representative MR hydrogels and the gelatin hydrogel with no microgels. When a relatively small amount of microgels was added (MR2.5-0.25 (MRx-y: GG concentration is x% in microgels and y% in MR hydrogels)), the modulus did not increase significantly, but the failure stress increased significantly (statistical analysis is shown in Figure 4.3. (C) and (D)). When a relatively large amount of microgels was added (MR2.5-1.0), both the modulus and the failure stress increased significantly, but the failure occurred at a lower strain resulting in not as high failure stress as in the previous formulation (statistical analysis is shown in Figure 4.3. (C) and (D). Figure 4.3. (C)

shows the compressive modulus of the all MR hydrogel formulations prepared. GG1.0 microgels were not stiff enough so that adding them with up to 1% GG concentration in MR hydrogel did not make significant increase in the compressive modulus of the MR hydrogels. GG1.5, GG2.0, and GG2.5 microgels did not increase the compressive modulus of the MR hydrogels significantly at only 0.25% GG concentration in MR hydrogel, however, at more than 0.25%, as more amount of the microgels were added, the modulus of MR hydrogels increased. At higher GG concentrations (0.75% and 1%) in MR hydrogel, GG2.5, which is the stiffest microgels, resulted in highest compressive modulus among the all microgel formulations. Figure 4.3. (D) shows that all formulations of MR hydrogels prepared exhibited higher strength than the gelatin hydrogels. When the microgels of the highest GG concentration (GG2.5) were added, the failure stress abruptly increased at the lowest GG concentration in MR hydrogel (0.25%), and it clearly decreased as the GG concentration in MR hydrogel increased. The maximal strength was 3.2MPa, which was 2.8 times that of the gelatin hydrogels. However, as the GG concentration of the microgels decreased, the failure stress at the lowest GG concentration in MR hydrogel decreased, and it did not decrease as much with the increase of the GG concentration in MR hydrogel. At 1% GG concentration in MR hydrogel, MR hydrogels with GG1.0 showed even higher strength than those with GG2.5. The strengthening mechanism of MR hydrogels has been previously elucidated: the GG microgels provides additional crosslinkers that can ultimately resist the crack propagation in the gelatin network [56]. Although the GG microgels are brittle, so cracks can grow in the microgels, the microgels are dispersed in the gelatin network so the cracks of microgels do not propagate into macroscopic ones until the crack of gelatin network starts to grow.

Comparison with DN hydrogels from the same two polymers with MR hydrogels showed that MR hydrogels have significantly higher strength. The compressive modulus and the failure stress of a DN hydrogel were showed in each dotted box in Figure 4.3. (C) and (D). The formulation of the DN hydrogel was 0.5% GG / 10% gelatin, which is optimal for high strength at 10% gelatin concentration. If the GG concentration increases, the modulus becomes much higher, but the failure stress decreases.[163] But, even with the optimal formulation, the failure stress of the DN hydrogels is only 1.4 times that of the gelatin hydrogels. In previous work, the

DN hydrogels were prepared from GG and gelatin solutions in distilled water. However, it turned out that the DN hydrogels prepared from the GG solution in PBS and the gelatin solution in media, which are cell-compatible solutions, exhibited significantly lower strength than those prepared from water solution. We determined that this is because the GG molecules collapse when they are in a solution with high ionic strength such as PBS or media. GG molecules have negative charges on their backbone, so they exist as extended form in distilled water due to the repulsive force between the charges. However, when they are in a solution with many ions, the electric interactions are screened by the ions and the molecules collapse.[168, 169] The MR hydrogels were also prepared from gelatin solutions with GG microgels in PBS, so the strength might be lower than that of the MR hydrogels prepared form water solutions, but the higher GG concentration of the microgels (thus higher stiffness of microgels) enhanced the strength of the MR hydrogels, which was not the case for the DN hydrogels. This is the mechanical advantage of the MR hydrogels over DN hydrogels.

To investigate the microstructure of the hydrogels, SEM images of the cross-section of the GG, gelatin, DN and MR1.5-1.0 hydrogels were taken (Figure 4.4). All the hydrogels presented interconnected porous structure, which accelerates the transport of nutrients and waste products. However, except for GG hydrogels, the pore size of the hydrogels was less than 10μm, which might not be big enough, so the cell growth and migration in the hydrogels might be impeded. Thus, some degradation of the hydrogels might be needed to facilitate cell behaviors and the formation of extracellular matrix.

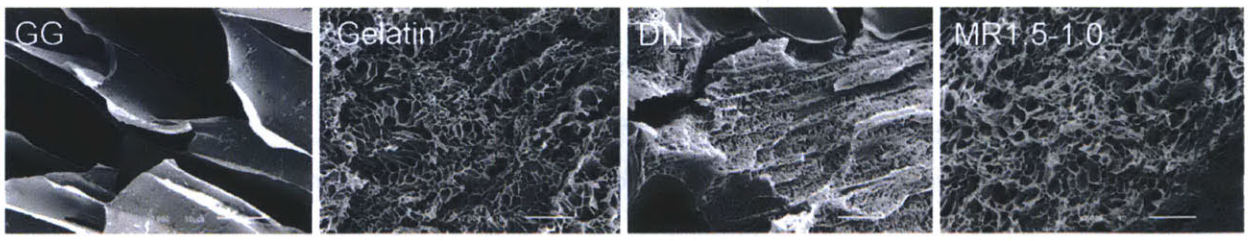

Figure 4.4. SEM images of cross-section of hydrogels. The scale bars represent 10μm.

4.3.3. Cell behavior in MR hydrogels

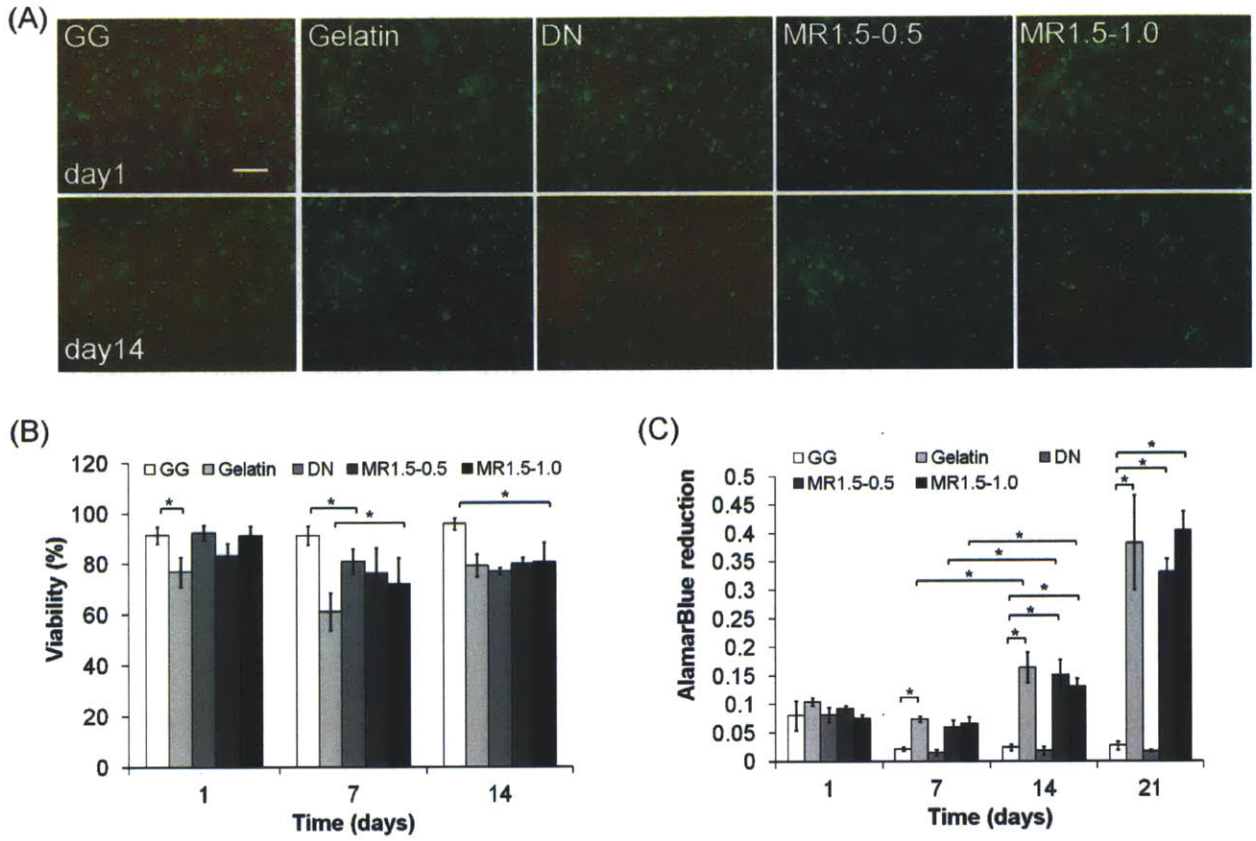

Figure 4.5. (A) Live/dead staining on MC3T3-E1 cells / hydrogel constructs after 1 and 14 days in culture. The scale bar represents 100μm.(B) Viability and (C) metabolic activity (AlamarBlue assay) of MC3T3-E1 cells encapsulated in hydrogels after culture. (*) indicates significant difference ($p<0.05$).

The MC3T3-E1 cell line is a preosteoblast derived from *Mus musculus* (mouse) calvaria.[170] It has been widely used as a model to evaluate the capacity of substrates for osteogenic differentiation.[171-173] It exhibits high levels of differentiation after culture in media with ascorbic acid and phosphate producing osteogenic markers such as ALP and depositing minerals.[174-176] We encapsulated these cells in five hydrogel formulations which are GG, gelatin, DN, MR1.5-0.5, MR1.5-1.0 (MRx-y: GG concentration is x% in microgels and y% in MR hydrogels) hydrogels. The images of the calcein AM/ethidium homodimer-1 live/dead stained hydrogels are shown in Figure 4.5. (A). At all formulations of hydrogels, the cell viability was over 70% after 14 days of culture (Figure 4.5. (B)), which is on par with typical photocrosslinked hydrogels.[13, 37, 39] This shows that the photocrosslinking conditions such as the intensity of the

light, the exposure time and the photoinitiator concentration were well adjusted for the MC3T3-E1 cells. The microgels contained negligible amount of toxic chemicals that could harm cells, and the microgels themselves were not harmful to cells. In addition, requirements for cell survival such as the transport of nutrients and wastes were met. It is presumed that the higher viability in the GG hydrogels than that in other hydrogels at day 7 and 14 is because the initial damage by the photocrosslinking was less in GG hydrogels due to more amount of methacrylate groups which can react with free radicals that is harmful to cells.[13] It was observed that higher concentration of the photoinitiator led to even lower viability in the gelatin hydrogels, while the viability remained at the same level in the GG hydrogels (data not shown). However, the metabolic activity of the cells showed significant difference between varying formulations as seen in Figure 4.5. (C). In the gelatin and the two MR hydrogels, the metabolic activity started to increase at day 14, and ended up with about four-fold increase at day 21 compared to day 1. However, the metabolic activity in the GG and the DN hydrogels significantly decreased at day 7, and remained low until day 21. The difference between these two groups was that the cells were encapsulated in gelatin for the former group, while the cells were encapsulated in GG for the latter group. The MC3T3-E1 cells are anchorage-dependent cells of which the activity, function, and differentiation are highly affected by the adhesion to a substrate.[177, 178] It is well known that gelatin is a great material for this kind of cells because it has many adhesion sites such as RGD peptide.[20] Thus the higher metabolic activity in the former group is presumed that because MC3T3-E1 cells were better attached to the gelatin environment than to the GG environment. Although gelatin molecules penetrated into the GG hydrogel so the cells might face partly the gelatin environment in DN hydrogels, it is speculated that the gelatin could not strongly interact with the cells when the cells were already stuck in the GG network. Seeing that the level of the metabolic activity in the gelatin, MR1.5-0.5, and MR1.5-1.0 hydrogels were all similar, it is concluded that the GG microgels did not interfere significantly with the cell-gelatin interaction at up to 1.0% concentration.

The level of the osteogenic behavior of the MC3T3-E1 cells in each hydrogel formulation was assessed by examining ALP activity and mineralization. As seen in Figure 4.6, ALP activity in

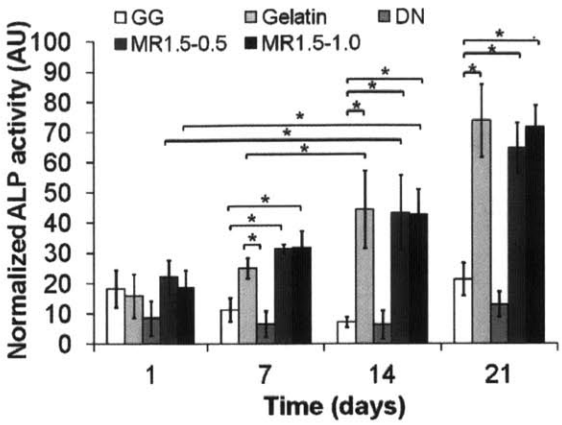

Figure 4.6. Alkaline phosphatase expression of MC3T3-E1 cells normalized by the amount of DNA after culture. (*) indicates significant difference ($p<0.05$).

the gelatin and the two MR hydrogels again increased significantly over 21 days of culture, while that in the GG and DN hydrogels remained significantly lower. It is most likely because of the same reason as the difference in metabolic activity, the cell-gelatin interaction. The facilitation of the differentiation of MC3T3-E1 cells or osteogenic differentiation of mesenchymal stem cells (MSCs) by using a cell-adhesive substrate has been shown in previous studies.[178-180] The enhanced osteogenic behavior in the gelatin and MR hydrogels was also confirmed by the Alizarin Red S staining for minerals (Figure 4.7, 4.8). At day 28 of culture, all the surface of the gelatin and the MR hydrogels turned red, while the GG and DN hydrogels still have unstained areas (Figure 4.7). Quantitative analysis in Figure 4.8 shows that adding up to 1% of GG microgels into gelatin hydrogels did not affect the amount of the mineralization significantly. Although the amounts of Alizarin Red S stained in the constructs increased at day 21 in all hydrogel formulations compared to those at day 1, the gelatin and the two MR hydrogels contained significantly higher amount of Alizarin Red S than the GG and the DN hydrogels at day 21 and 28. These results show that the MR hydrogel is a better system than the DN hydrogel in perspective of biological properties as well. However, it should be noted that depending on the properties of the cells encapsulated, the effect of the hydrogel formulation on the function or the differentiation of the cells can be different. For example, RGD peptides that exist on gelatin molecules promote early stages of chondrogenesis of MSCs, but their persistence in the scaffold can limit complete differentiation of MSCs.[181, 182] Thus, the

properties of the cells always need to be considered when a hydrogel formulation is selected for a certain purpose. Finding other materials that have different biological properties and can be used as the stiff reinforcing microgels or the soft and ductile matrix will thus broaden the range of applications of MR hydrogels.

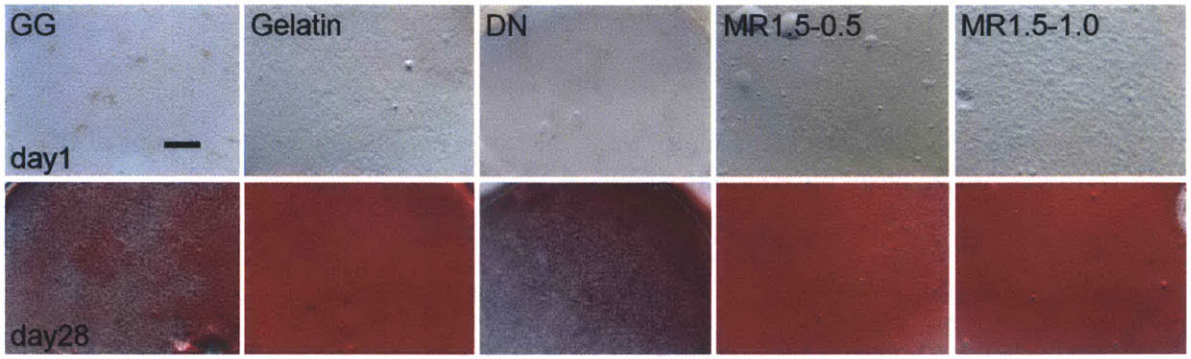

Figure 4.7. Alizarin Red S staining on MC3T3-E1 cells / hydrogel constructs after 1 and 28 days in culture. The scale bar represents 500μm.

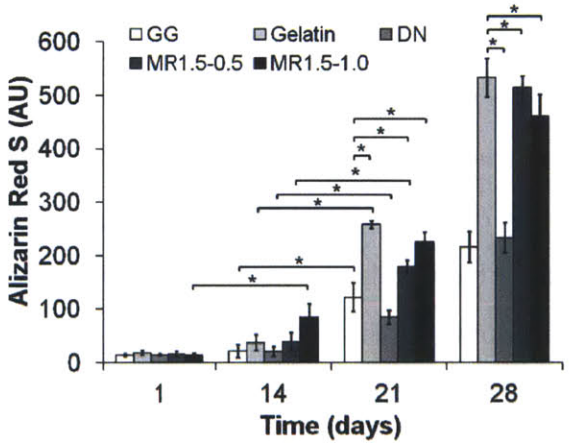

Figure 4.8. Quantification of Alizarin Red S stained in MC3T3-E1 cells / hydrogel constructs. (*) indicates significant difference ($p<0.05$).

Finally, another advantage of MR hydrogels as tissue scaffolds is that they are potentially injectable as previously studied photocrosslinkable polymers,[93, 183] which is not the case for DN hydrogels. By adding the GG component in the gelatin hydrogels as microgels not as bulk hydrogels, injection of the gelatin solutions with GG microgels and cells into a body

followed by a photocrosslinking *in situ* became possible. This enables the minimally invasive implantation, which is one of the advantages of hydrogel-based tissue scaffolds over those from different types of material.[8, 93, 184] However, it should be noted that, although the feasibility of photocrosslinking of injected polymers in vivo by transdermal light exposure was confirmed,[185] further studies to overcome inefficient light penetration through skin and develop biocompatible photoinitiator are needed for clinical use as injectable tissue scaffolds.

4.4. Conclusions

We developed mechanically strong MR hydrogels by embedding stiff GG microgels into soft and ductile gelatin hydrogels. The MR hydrogels exhibited higher strength than the DN hydrogels and the gelatin hydrogels with no microgels. The strength of MR hydrogels varied with the polymer concentration in the GG microgels and the GG concentration in the MR hydrogels. MC3T3-E1 preosteoblasts were encapsulated in the MR hydrogels with a high cell viability. They exhibited as high metabolic activity in the MR hydrogels as in the gelatin hydrogels after culture, while their metabolic activity remained low over time in the DN hydrogels. The osteogenic behavior determined by measuring ALP activity and mineralization was facilitated as greatly in the MR hydrogels as in the gelatin hydrogels, while the osteogenic behavior was not as facilitated in DN hydrogels. These results suggest that the MR hydrogels may have high potential as load-bearing tissue scaffolds.

Chapter 5: Conclusions and future research

5.1. Summary

The development of scaffolds with biomimetic mechanical and biological properties is a critical part in tissue engineering. Hydrogels are promising candidates for tissue engineering scaffold due to their properties that are similar to native tissues, but its mechanical weakness is a main challenge that limits its use as tissue scaffolds. Thus, the work in this thesis focused on the development of cell-laden hydrogels with high mechanical strength and great biological activity as potential tissue engineering scaffolds.

In the first work (Chapter 2), a hydrophilic, biodegradable polymer, poly(glucose malate)methacrylate (PGMma), was synthesized from two monomers, glucose and malic acid, which are found in the human metabolic system, by a polycondensation reaction followed by modification with the photoreactive methacrylate groups. By altering the ratio of the staring monomers and the degree of methacrylation, mechanical properties, swelling, and degradation rate of the resulting hydrogels could be tuned, the failure stress reaching up to ~0.2 MPa. NIH 3T3 fibroblasts attached and proliferated on the PGMma hydrogels, which suggested that the PGMma hydrogels could be potentially useful for tissue scaffolds.

In the second work (Chapter 3), cell-laden double-network (DN) hydrogels with high mechanical strength were developed from two photocrosslinkable biomacromolecules, gellan gum (GG) and gelatin, by using a cell-compatible two-step photocrosslinking. The resulting DN hydrogels exhibited higher strength than GG or gelatin single-network hydrogels, the maximal failure stress being 6.9 MPa. An optimal range of the degree of methacrylation of the second polymer existed for maximal strength of the DN hydrogels, and higher mass ratio of gelatin/GG resulted in stronger DN hydrogels. The high viability of NIH 3T3 fibroblasts after encapsulation in DN hydrogels indicated that the DN formation process was cell-compatible.

In the last work (Chapter 4), cell-laden microgel-reinforced (MR) hydrogels were developed by embedding GG microgels into gelatin hydrogels. The resulting MR hydrogels exhibited higher strength than the DN hydrogels and gelatin hydrogels with no microgels, the maximal strength being 2.8 times that of the gelatin hydrogels. The strength of the MR

hydrogels was affected by the GG concentration in microgels and that in MR hydrogels. MC3T3-E1 preosteoblasts encapsulated in the MR hydrogels exhibited higher metabolic activity and ALP activity, and deposited more minerals than those in the DN hydrogels, which suggested that the MR hydrogels could be a better alternative to the DN hydrogels.

In conclusion, mechanically strong hydrogels that can encapsulate cells and also present suitable properties as tissue scaffolds were developed. They showed high potential especially as load-bearing tissue scaffolds. Most of the previous researches worked on either only developing strong hydrogels or only developing biocompatible hydrogels that facilitate cell behaviors, but in this work, hydrogels that showed both simultaneously was developed. This work also tells that when tissue scaffolds are designed, both physical and biological properties of materials need to be considered for the optimal formulation.

5.2. Future work

5.2.1. Enhancement of hydrogel strength

As explained in Chapter 4, the reason that the DN hydrogels weakened when they were prepared from cell-compatible solutions is that the GG molecules which have negative charges on the backbone collapse due to the screening of the electric repulsive force by ions in the solutions. Although not examined, it is likely that the MR hydrogels prepared from cell-compatible solutions also exhibit lower strength than those from water solutions with a negligible concentration of ions. Thus, attempts to find alternative biopolymers to GG that have no charges on the backbone are motivated, such as dextran or pullulan with molecular weights large enough to form stiff hydrogels at low concentrations. Since the intrinsic molecular structure and the thermodynamic interaction between different polymer molecules could affect the strength of the resulting hydrogels [54, 186], using alternative materials could lead to unexpected results.

A main reason for the mechanical disadvantage of photocrosslinked hydrogels is the inhomogeneous network structure [41]. Photocrosslinking occurs via a chain polymerization reaction of the carbon-carbon double bonds in which the chains propagates at limited number

of active sites resulting in inhomogeneous distribution of the large, multi-crosslinked chains. When a force is applied, stress is concentrated around dense crosslinks, and this leads to fracture of the hydrogels at low stress. Thus, attempts to achieve more homogeneous distribution of crosslinks are motivated. For example, the GG microgels could be prepared by using a small chemical crosslinker, or by attaching two different functional groups that react with each other on the GG molecules. Since GG microgels are prepared without cells, various chemical reactions would be possible. Cell-compatible chemical crosslinking is a significant challenge for network formations that encapsulate cells, thus developing a non-toxic chemical crosslinker is a good topic for future research.

In addition, previous studies on the effect of the particle size and the particle size distribution in the micrometer range on the mechanical properties of particle-polymer composites have shown that the strength of composites increases as the particle size decreases, while the particle size distribution does not have a clear effect on the strength [187-189]. The size of the GG microgels was several micrometers and they were very polydisperse. Although the system is different, it should be worthwhile to prepare GG microgels with different sizes and narrower size distribution and examine their effect on the strength of the MR hydrogels.

5.2.2. Further research needed for tissue formation

Although the NIH 3T3 fibroblasts and the MC3T3-E1 preosteoblasts were encapsulated in hydrogels by photocrosslinking without critical damage, the effect of light or photoinitiator may differ for other cells. Even for MC3T3-E1 cells were needed more mild conditions than for NIH 3T3 cells. Thus, for specific applications, the optimal photocrosslinking conditions needs to be found for the specific cells. If the cells are too vulnerable to photocrosslinking, compromise in the strength of hydrogels is inevitable. Furthermore, even if the cells encapsulated by photocrosslinking exhibits high viability, it is difficult to conclude that the cells remain in their biological integrity, for example, there is no damage of DNA, RNA, or other molecules that are critical to the fate or function of the cells. So far not many studies have demonstrated that photocrosslinking does not harm the biological integrity of the encapsulated cells. Future

research should focus on more extensive experiments to investigate the effect of photocrosslinking on cells.

Degradation rate is also a critical factor for successful scaffolds. If the hydrogels degrade too fast, they will lose the strength too soon. Thus researches on whether the degradation rate is adequate compared to the ECM formation rate are required to use the strong hydrogels in real applications. Controlling the crosslink density or mixing with other materials that have different degradation rate or degradation mechanism is likely the easiest way to tune the degradation rate. Designing smart materials such as the recently developed synthetic material of which the degradation depend on the cell-material interaction [190, 191] may be a powerful strategy in the future research to control the degradation rate.

Pore size should be considered as well to improve the hydrogel scaffolds. Conventional hydrogels have small pore size limiting cell growth, ECM production, and neovascularization [63, 192]. One approach to overcome this is to create microcavities inside hydrogels which lead to spontaneous outgrowth of cells into the microcavities from the cell-laden hydrogels [192]. However, this could affect the strength of the hydrogels, so balancing the amount of microcavities and the strength is needed. Cell-responsive hydrogels could be another strategy, which does not lead to decrease in strength [191].

Finally, since light needs to reach to the crosslinking sites to initiate the reaction, limitation exists in the thickness of photocrosslinked hydrogels. If the hydrogels are too thick, the degree of crosslinking decreases with the distance from the surface of hydrogels. This is another drawback of photocrosslinked hydrogels and the reason that other non-toxic chemical crosslinking methods are needed. If cell-laden strong hydrogels with larger volumes are prepared, vascularization in the construct becomes more important. Vascularization is needed to supply nutrients and oxygen to cells, and actually it is a major hurdle for all the cell-laden tissue constructs. In order to accelerate the formation of vascular networks, several strategies have been developed, such as microfabrication of vascular geometry [193-195], addition of angiogenic growth factors [196-198], and co-culture of endothelial cells with osteoblasts [199-201]. Combining these strategies with the MR hydrogel approach may facilitate the tissue formation in the strong hydrogels.

References

1. R. Langer and J. Vacanti, *Science*, 1993, **260**, 920-926.
2. L. G. Griffith and G. Naughton, *Science Signaling*, 2002, **295**, 1009.
3. P. Bianco and P. G. Robey, *Nature*, 2001, **414**, 118-121.
4. J. E. Babensee, L. V. McIntire and A. G. Mikos, *Pharmaceutical research*, 2000, **17**, 497-504.
5. D. W. Hutmacher, *Biomaterials*, 2000, **21**, 2529-2543.
6. S. Yang, K.-F. Leong, Z. Du and C.-K. Chua, *Tissue Engineering*, 2001, **7**, 679-689.
7. L. S. Nair and C. T. Laurencin, in *Tissue Engineering I*, Springer, 2006, pp. 47-90.
8. J. L. Drury and D. J. Mooney, *Biomaterials*, 2003, **24**, 4337-4351.
9. K. Lee and D. Mooney, *Chemical reviews*, 2001, **101**, 1869-1880.
10. M. D. Brigham, A. Bick, E. Lo, A. Bendali, J. A. Burdick and A. Khademhosseini, *Tissue Engineering Part A*, 2009, **15**, 1645-1653.
11. J. A. Rowley, G. Madlambayan and D. J. Mooney, *Biomaterials*, 1999, **20**, 45-53.
12. S. Bryant, C. Nuttelman and K. Anseth, *Journal of Biomaterials Science, Polymer Edition*, 2000, **11**, 439-457.
13. N. E. Fedorovich, M. H. Oudshoorn, D. van Geemen, W. E. Hennink, J. Alblas and W. J. A. Dhert, *Biomaterials*, 2009, **30**, 344-353.
14. A. Khademhosseini and R. Langer, *Biomaterials*, 2007, **28**, 5087-5092.
15. J. Ifkovits and J. Burdick, *Tissue Engineering*, 2007, **13**, 2369-2385.
16. H. Qi, Y. Du, L. Wang, H. Kaji, H. Bae and A. Khademhosseini, *Advanced Material*, 2010, **22**, 5276-5281.
17. W. T. Brinkman, K. Nagapudi, B. S. Thomas and E. L. Chaikof, *Biomacromolecules*, 2003, **4**, 890-895.
18. C.-M. Dong, X. Wu, J. Caves, S. S. Rele, B. S. Thomas and E. L. Chaikof, *Biomaterials*, 2005, **26**, 4041-4049.
19. J. A. Benton, C. A. DeForest, V. Vivekanandan and K. S. Anseth, *Tissue Engineering Part A*, 2009, **15**, 3221-3230.
20. J. W. Nichol, S. T. Koshy, H. Bae, C. M. Hwang, S. Yamanlar and A. Khademhosseini, *Biomaterials*, 2010, **31**, 5536-5544.
21. H. Okino, Y. Nakayama, M. Tanaka and T. Matsuda, *Journal of biomedical materials research*, 2002, **59**, 233-245.
22. B. G. Amsden, A. Sukarto, D. K. Knight and S. N. Shapka, *Biomacromolecules*, 2007, **8**, 3758-3766.
23. M. Ishihara, K. Obara, T. Ishizuka, M. Fujita, M. Sato, K. Masuoka, Y. Saito, H. Yura, T. Matsui and H. Hattori, *Journal of Biomedical Materials Research Part A*, 2003, **64**, 551-559.
24. O. Jeon, K. H. Bouhadir, J. M. Mansour and E. Alsberg, *Biomaterials*, 2009, **30**, 2724-2734.
25. A. I. Chou and S. B. Nicoll, *Journal of Biomedical Materials Research Part A*, 2009, **91**, 187-194.
26. J. Trudel and S. Massia, *Biomaterials*, 2002, **23**, 3299-3307.
27. P. Matricardi, M. Pontoriero, T. Coviello, M. A. Casadei and F. Alhaique, *Biomacromolecules*, 2008, **9**, 2014-2020.
28. Y. Liu and M. B. Chan-Park, *Biomaterials*, 2009, **30**, 196-207.
29. J. B. Leach and C. E. Schmidt, *Biomaterials*, 2005, **26**, 125-135.
30. A. Khademhosseini, G. Eng, J. Yeh, J. Fukuda, J. Blumling, R. Langer and J. A. Burdick, *Journal of Biomedical Materials Research Part A*, 2006, **79**, 522-532.
31. J. Kim, I. S. Kim, T. H. Cho, K. B. Lee, S. J. Hwang, G. Tae, I. Noh, S. H. Lee, Y. Park and K. Sun, *Biomaterials*, 2007, **28**, 1830-1837.
32. I. Levental, P. C. Georges and P. A. Janmey, *Soft Matter*, 2007, **3**, 299-306.
33. Y. Fung, *Biomechanics: mechanical properties of living tissues*, Springer, 1993.

34. A. K. Williamson, A. C. Chen, K. Masuda, E. J. Thonar and R. L. Sah, *Journal of Orthopaedic Research*, 2003, **21**, 872-880.
35. T. A. Wren, S. A. Yerby, G. S. Beaupre and D. R. Carter, *Clinical Biomechanics*, 2001, **16**, 245-251.
36. J.-Y. Rho, L. Kuhn-Spearing and P. Zioupos, *Medical engineering & physics*, 1998, **20**, 92-102.
37. J. Burdick, C. Chung, X. Jia, M. Randolph and R. Langer, *Biomacromolecules*, 2005, **6**, 386-391.
38. D. F. Coutinho, S. V. Sant, H. Shin, J. T. Oliveira, M. E. Gomes, N. M. Neves, A. Khademhosseini and R. L. Reis, *Biomaterials*, 2010, **31**, 7494-7502.
39. H. Bae, A. F. Ahari, H. Shin, J. W. Nichol, C. B. Hutson, M. Masaeli, S. H. Kim, H. Aubin, S. Yamanlar and A. Khademhosseini, *Soft Matter*, 2011, **7**, 1903-1911.
40. S. J. Bryant, R. J. Bender, K. L. Durand and K. S. Anseth, *Biotechnology and bioengineering*, 2004, **86**, 747-755.
41. J. Gong, *Soft Matter*, 2010, **6**, 2583-2590.
42. T. Sakai, T. Matsunaga, Y. Yamamoto, C. Ito, R. Yoshida, S. Suzuki, N. Sasaki, M. Shibayama and U. I. Chung, *Macromolecules*, 2008, **41**, 5379-5384.
43. Y. Okumura and K. Ito, *Advanced Materials*, 2001, **13**, 485-487.
44. K. Haraguchi and T. Takehisa, *Advanced Materials*, 2002, **14**, 1120-1124.
45. K. J. Henderson, T. C. Zhou, K. J. Otim and K. R. Shull, *Macromolecules*, 2010, **43**, 6193-6201.
46. M. J. Glassman, J. Chan and B. D. Olsen, *Advanced Functional Materials*, 2013, **23**, 1182-1193.
47. J. Gong, Y. Katsuyama, T. Kurokawa and Y. Osada, *Advanced Materials*, 2003, **15**, 1155-1158.
48. D. J. Waters, K. Engberg, R. Parke-Houben, C. N. Ta, A. J. Jackson, M. F. Toney and C. W. Frank, *Macromolecules*, 2011, **44**, 5776-5787.
49. A. Nakayama, A. Kakugo, J. P. Gong, Y. Osada, M. Takai, T. Erata and S. Kawano, *Advanced Functional Materials*, 2004, **14**, 1124-1128.
50. D. Myung, W. Koh, J. Ko, J. Noolandi, M. Carrasco, A. Smithc, C. Frank and C. Ta, *Investigative Ophthalmology & Visual Science*, 2005, **46**, 1.
51. Y. H. Na, T. Kurokawa, Y. Katsuyama, H. Tsukeshiba, J. P. Gong, Y. Osada, S. Okabe, T. Karino and M. Shibayama, *Macromolecules*, 2004, **37**, 5370-5374.
52. Q. M. Yu, Y. Tanaka, H. Furukawa, T. Kurokawa and J. P. Gong, *Macromolecules*, 2009, **42**, 3852-3855.
53. H. Tsukeshiba, M. Huang, Y.-H. Na, T. Kurokawa, R. Kuwabara, Y. Tanaka, H. Furukawa, Y. Osada and J. P. Gong, *The Journal of Physical Chemistry B*, 2005, **109**, 16304-16309.
54. M. Huang, H. Furukawa, Y. Tanaka, T. Nakajima, Y. Osada and J. P. Gong, *Macromolecules*, 2007, **40**, 6658-6664.
55. T. Nakajima, H. Furukawa, Y. Tanaka, T. Kurokawa and J. P. Gong, *Journal of Polymer Science Part B: Polymer Physics*, 2011, **49**, 1246-1254.
56. J. Hu, K. Hiwatashi, T. Kurokawa, S. M. Liang, Z. L. Wu and J. P. Gong, *Macromolecules*, 2011, **44**, 7775-7781.
57. J. Hu, T. Kurokawa, K. Hiwatashi, T. Nakajima, Z. L. Wu, S. M. Liang and J. P. Gong, *Macromolecules*, 2012, **45**, 5218-5228.
58. X. P. Qin, F. Zhao, Y. K. Liu, H. Y. Wang and S. Y. Feng, *Colloid Polym. Sci.*, 2009, **287**, 621-625.
59. S. Lally, R. Liu, C. Supasuteekul, B. R. Saunders and T. Freemont, *Journal of Materials Chemistry*, 2011, **21**, 17719-17728.
60. A. K. Jha, M. S. Malik, M. C. Farach-Carson, R. L. Duncan and X. Jia, *Soft Matter*, 2010, **6**, 5045-5055.
61. D. Sommerfeldt and C. Rubin, *European Spine Journal*, 2001, **10**, S86-S95.
62. V. I. Sikavitsas, J. S. Temenoff and A. G. Mikos, *Biomaterials*, 2001, **22**, 2581-2593.
63. A. n. J. Salgado, O. P. Coutinho and R. L. Reis, *Macromolecular bioscience*, 2004, **4**, 743-765.
64. B. Sharma and J. H. Elisseeff, *Annals of biomedical engineering*, 2004, **32**, 148-159.

65. C. A. Heath, *Trends in biotechnology*, 2000, **18**, 17-19.
66. L. Buttery, S. Bourne, J. Xynos, H. Wood, F. Hughes, S. Hughes, V. Episkopou and J. Polak, *Tissue Engineering*, 2001, **7**, 89-99.
67. A. I. Caplan, *Journal of Orthopaedic Research*, 1991, **9**, 641-650.
68. S. J. Peter, C. R. Liang, D. J. Kim, M. S. Widmer and A. G. Mikos, *Journal of cellular biochemistry*, 1998, **71**, 55-62.
69. N. Jaiswal, S. E. Haynesworth, A. I. Caplan and S. P. Bruder, *Journal of cellular biochemistry*, 1997, **64**, 295-312.
70. C. Szpalski, M. Barbaro, F. Sagebin and S. M. Warren, *Tissue Engineering Part B: Reviews*, 2012, **18**, 258-269.
71. R. Quarto, M. Mastrogiacomo, R. Cancedda, S. M. Kutepov, V. Mukhachev, A. Lavroukov, E. Kon and M. Marcacci, *New England Journal of Medicine*, 2001, **344**, 385-386.
72. C. A. Vacanti, L. J. Bonassar, M. P. Vacanti and J. Shufflebarger, *New England Journal of Medicine*, 2001, **344**, 1511-1514.
73. M. Grynpas, R. Pilliar, R. Kandel, R. Renlund, M. Filiaggi and M. Dumitriu, *Biomaterials*, 2002, **23**, 2063-2070.
74. J. Dong, T. Uemura, Y. Shirasaki and T. Tateishi, *Biomaterials*, 2002, **23**, 4493-4502.
75. M. M. Stevens, *Materials today*, 2008, **11**, 18-25.
76. H. Ueda, L. Hong, M. Yamamoto, K. Shigeno, M. Inoue, T. Toba, M. Yoshitani, T. Nakamura, Y. Tabata and Y. Shimizu, *Biomaterials*, 2002, **23**, 1003-1010.
77. E. Sachlos, N. Reis, C. Ainsley, B. Derby and J. Czernuszka, *Biomaterials*, 2003, **24**, 1487-1497.
78. X. B. Yang, R. S. Bhatnagar, S. Li and R. O. Oreffo, *Tissue Engineering*, 2004, **10**, 1148-1159.
79. J. Patterson, R. Siew, S. W. Herring, A. S. P. Lin, R. Guldberg and P. S. Stayton, *Biomaterials*, 2010, **31**, 6772-6781.
80. H. D. Kim and R. F. Valentini, *Journal of biomedical materials research*, 2002, **59**, 573-584.
81. G. Lisignoli, N. Zini, G. Remiddi, A. Piacentini, A. Puggioli, C. Trimarchi, M. Fini, N. M. Maraldi and A. Facchini, *Biomaterials*, 2001, **22**, 2095-2105.
82. L. Meinel, V. Karageorgiou, S. Hofmann, R. Fajardo, B. Snyder, C. Li, L. Zichner, R. Langer, G. Vunjak-Novakovic and D. L. Kaplan, *Journal of Biomedical Materials Research Part A*, 2004, **71**, 25-34.
83. C. Li, C. Vepari, H.-J. Jin, H. J. Kim and D. L. Kaplan, *Biomaterials*, 2006, **27**, 3115-3124.
84. L. Meinel, S. Hofmann, O. Betz, R. Fajardo, H. P. Merkle, R. Langer, C. H. Evans, G. Vunjak-Novakovic and D. L. Kaplan, *Biomaterials*, 2006, **27**, 4993.
85. N. Saito, T. Okada, H. Horiuchi, N. Murakami, J. Takahashi, M. Nawata, H. Ota, K. Nozaki and K. Takaoka, *Nature Biotechnology*, 2001, **19**, 332-335.
86. R. C. Thomson, A. G. Mikos, E. Beahm, J. C. Lemon, W. C. Satterfield, T. B. Aufdemorte and M. J. Miller, *Biomaterials*, 1999, **20**, 2007-2018.
87. J. M. Karp, M. S. Shoichet and J. E. Davies, *Journal of Biomedical Materials Research Part A*, 2003, **64A**, 388-396.
88. D. Rohner, D. W. Hutmacher, T. K. Cheng, M. Oberholzer and B. Hammer, *Journal of Biomedical Materials Research Part B*, 2003, **66B**, 574-580.
89. H. Yoshimoto, Y. M. Shin, H. Terai and J. P. Vacanti, *Biomaterials*, 2003, **24**, 2077-2082.
90. M. Shin, H. Yoshimoto and J. P. Vacanti, *Tissue Engineering*, 2004, **10**, 33-41.
91. J. M. Williams, A. Adewunmi, R. M. Schek, C. L. Flanagan, P. H. Krebsbach, S. E. Feinberg, S. J. Hollister and S. Das, *Biomaterials*, 2005, **26**, 4817-4827.
92. C. R. Nuttelman, M. C. Tripodi and K. S. Anseth, *Journal of Biomedical Materials Research Part A*, 2004, **68**, 773-782.
93. J. A. Burdick and K. S. Anseth, *Biomaterials*, 2002, **23**, 4315-4323.

94. D. S. Benoit, A. R. Durney and K. S. Anseth, *Biomaterials*, 2007, **28**, 66-77.
95. C. Rodrigues, P. Serricella, A. Linhares, R. Guerdes, R. Borojevic, M. Rossi, M. Duarte and M. Farina, *Biomaterials*, 2003, **24**, 4987-4997.
96. F. Zhao, Y. Yin, W. W. Lu, J. C. Leong, W. Zhang, J. Zhang, M. Zhang and K. Yao, *Biomaterials*, 2002, **23**, 3227-3234.
97. Y. Zhang, J. R. Venugopal, A. El-Turki, S. Ramakrishna, B. Su and C. T. Lim, *Biomaterials*, 2008, **29**, 4314-4322.
98. Y.-M. Lee, Y.-J. Park, S.-J. Lee, Y. Ku, S.-B. Han, P. R. Klokkevold, S.-M. Choi and C.-P. Chung, *Journal of periodontology*, 2000, **71**, 410-417.
99. H. M. Nie and C. H. Wang, *Journal of Controlled Release*, 2007, **120**, 111-121.
100. N. Peppas and R. Langer, *Science*, 1994, **263**, 1715-1720.
101. R. Langer and J. Vacanti, *Science*, 1993, **260**, 920-926.
102. Y. Wang, G. Ameer, B. Sheppard and R. Langer, *Nature Biotechnology*, 2002, **20**, 602-606.
103. J. Yang, A. Webb and G. Ameer, *Advanced Materials*, 2004, **16**, 511-516.
104. C. Bettinger, J. Bruggeman, J. Borenstein and R. Langer, *Biomaterials*, 2008, **29**, 2315-2325.
105. H. Younes, E. Bravo-Grimaldo and B. Amsden, *Biomaterials*, 2004, **25**, 5261-5269.
106. J. Guan and W. Wagner, *Biomacromolecules*, 2005, **6**, 2833-2842.
107. J. Dey, H. Xu, J. Shen, P. Thevenot, S. Gondi, K. Nguyen, B. Sumerlin, L. Tang and J. Yang, *Biomaterials*, 2008, **29**, 4637-4649.
108. J. Bruggeman, C. Bettinger, C. Nijst, D. Kohane, R. Langer, J. Stichting and S. Fonds, *Advanced Materials*, 2008, **20**, 1922-1927.
109. J. Bruggeman, B. de Bruin, C. Bettinger and R. Langer, *Biomaterials*, 2008, **29**, 4726-4735.
110. K. Lee and D. Mooney, *Chemical Reviews*, 2001, **101**, 1869.
111. N. Peppas, J. Hilt, A. Khademhosseini and R. Langer, *Advanced Materials*, 2006, **18**, 1345.
112. A. Khademhosseini, J. P. Vacanti and R. Langer, *Scientific American*, 2009, **300**, 64-71.
113. A. Khademhosseini, R. Langer, J. Borenstein and J. P. Vacanti, *Proceedings of the National Academy of Sciences of the United States of America*, 2006, **103**, 2480-2487.
114. S. X. Lu and K. S. Anseth, *Journal of Controlled Release*, 1999, **57**, 291-300.
115. A. Kidane, J. M. Szabocsik and K. Park, *Biomaterials*, 1998, **19**, 2051-2055.
116. R. A. Stile, W. R. Burghardt and K. E. Healy, *Macromolecules*, 1999, **32**, 7370-7379.
117. C. S. Brazel and N. A. Peppas, *Journal of Controlled Release*, 1996, **39**, 57-64.
118. R. Schmedlen, K. Masters and J. West, *Biomaterials*, 2002, **23**, 4325-4332.
119. C. Nuttelman, S. Henry and K. Anseth, *Biomaterials*, 2002, **23**, 3617-3626.
120. K. Anseth, A. Metters, S. Bryant, P. Martens, J. Elisseeff and C. Bowman, *Journal of Controlled Release*, 2002, **78**, 199-209.
121. A. Sawhney, C. Pathak and J. Hubbell, *Macromolecules*, 1993, **26**, 581-587.
122. A. Metters, K. Anseth and C. Bowman, *Polymer*, 2000, **41**, 3993-4004.
123. M. Rice and K. Anseth, *Journal of Biomedical Materials Research Part A*, 2004, **70**, 560-568.
124. J. West and J. Hubbell, *Macromolecules*, 1999, **32**, 241-244.
125. Y. Poon, Y. Cao, Y. Zhu, Z. Judeh and M. Chan-Park, *Biomacromolecules*, 2009, **10**, 2043-2052.
126. B. He, E. Wan and M. Chan-Park, *Chemistry of Mater*ials, 2006, **18**, 3946-3955.
127. B. Lee, M. Fujita, N. Khazenzon, K. Wawrowsky, S. Wachsmann-Hogiu, D. Farkas, K. Black, J. Ljubimova and E. Holler, *Bioconjugate Chem*istry, 2006, **17**, 317-326.
128. J. Burdick, C. Chung, X. Jia, M. Randolph and R. Langer, *Biomacromolecules*, 2005, **6**, 386.
129. K. Smeds and M. Grinstaff, *Journal of Biomedical Materials Research*, 2001, **54**, 115-121.
130. J. Benton, C. DeForest, V. Vivekanandan and K. Anseth, *Tissue Engineering Part A*, 2009, **15**, 3221-3230.

131. A. Van Den Bulcke, B. Bogdanov, N. De Rooze, E. Schacht, M. Cornelissen and H. Berghmanss, *Biomacromolecules*, 2000, **1**, 31-38.
132. D. L. Hern and J. A. Hubbell, *Journal of Biomedical Materials Research*, 1998, **39**, 266-276.
133. P. D. Drumheller and J. A. Hubbell, *Analytical Biochemistry*, 1994, **222**, 380-388.
134. J. Berg, J. Tymoczko and L. Stryer, WH Freeman and Company. New York, 2002.
135. P. Flory, *Principles of polymer chemistry*, Cornell Univ Pr, 1953.
136. B. Amsden, *Soft Matter*, 2007, **3**, 1335-1348.
137. I. Levental, P. Georges and P. Janmey, *Soft Matter*, 2007, **3**, 299-306.
138. L. Nair and C. Laurencin, *Advances in Biochemical Engineering Biotechnology*, 2006, **102**, 47-90.
139. J. W. Nichol, S. T. Koshy, H. Bae, C. M. Hwang, S. Yamanlar and A. Khademhosseini, *Biomaterials*, 2010, **31**, 5536-5544.
140. X. Jia, J. Burdick, J. Kobler, R. Clifton, J. Rosowski, S. Zeitels and R. Langer, *Macromolecules*, 2004, **37**, 3239-3248.
141. S. Bencherif, A. Srinivasan, F. Horkay, J. Hollinger, K. Matyjaszewski and N. Washburn, *Biomaterials*, 2008, **29**, 1739-1749.
142. B. Amsden, A. Sukarto, D. Knight and S. Shapka, *Biomacromolecules*, 2007, **8**, 3758-3766.
143. A. J. Kerin, M. R. Wisnom and M. A. Adams, *Proceedings of the Institution of Mechanical Engineers Part H-Journal of Engineering in Medicine*, 1998, **212**, 273-280.
144. C. McCutchen, *Academic Press: New York*, 1978, **10**, 437.
145. P. Calvert, *Advanced Materials*, 2009, **21**, 743-756.
146. C. R. Nuttelman, M. A. Rice, A. E. Rydholm, C. N. Salinas, D. N. Shah and K. S. Anseth, *Progress in Polymer Science*, 2008, **33**, 167-179.
147. L. Weng, A. Gouldstone, Y. Wu and W. Chen, *Biomaterials*, 2008, **29**, 2153-2163.
148. D. F. Coutinho, S. V. Sant, H. Shin, J. T. Oliveira, M. E. Gomes, N. M. Neves, A. Khademhosseini and R. L. Reis, *Biomaterials*, 2010, **31**, 7494-7502
149. H. Bae, A. F. Ahari, H. Shin, J. W. Nichol, C. B. Hutson, M. Masaeli, S. H. Kim, H. Aubin, S. Yamanlar and A. Khademhosseini, *Soft Matter*, 2011, **7**, 1903-1911
150. J. Oliveira, L. Martins, R. Picciochi, P. Malafaya, R. Sousa, N. Neves, J. Mano and R. Reis, *Journal of Biomedical Materials Research Part A*, 2010, **93**, 852-863.
151. J. T. Oliveira, T. C. Santos, L. Martins, R. Picciochi, A. P. Marques, A. G. Castro, N. M. Neves, J. F. Mano and R. L. Reis, *Tissue Engineering Part A*, 2009, **16**, 343-353.
152. Y. Gong, C. Wang, R. C. Lai, K. Su, F. Zhang and D. Wang, *Journal of Materials Chemistry*, 2009, **19**, 1968-1977.
153. M. Hamcerencu, J. Desbrieres, A. Khoukh, M. Popa and G. Riess, *Carbohydrate Polymers*, 2008, **71**, 92-100.
154. F. Podczeck, *Pharmaceutical capsules*, Pharmaceutical Pr, 2004.
155. W. Jost, *Diffusion in solids, liquids, gases*, Academic Press New York, 1960.
156. R. Pawel, *Journal of Nuclear Materials*, 1974, **49**, 281-290.
157. P. Griffith, P. Stilbs, A. Howe and T. Cosgrove, *Langmuir*, 1996, **12**, 2884-2893.
158. T. Chang and H. Yu, *Macromolecules*, 1984, **17**, 115-117.
159. B. Amsden, *Macromolecules*, 1998, **31**, 8382-8395.
160. A. Pluen, P. A. Netti, R. K. Jain and D. A. Berk, *Biophysical journal*, 1999, **77**, 542-552.
161. T. Nakajima, H. Furukawa, Y. Tanaka, T. Kurokawa, Y. Osada and J. P. Gong, *Macromolecules*, 2009, **42**, 2184-2189.
162. N. Peppas, J. Hilt, A. Khademhosseini and R. Langer, *Advanced Materials*, 2006, **18**, 1345-1360.
163. H. Shin, B. D. Olsen and A. Khademhosseini, *Biomaterials*, 2012, **33**, 3143-3152.
164. J. Hu, T. Kurokawa, K. Hiwatashi, T. Nakajima, Z. L. Wu, S. M. Liang and J. P. Gong, *Macromolecules*, 2012, **45**, 5218-5228.

165. X. Q. Jia, Y. Yeo, R. J. Clifton, T. Jiao, D. S. Kohane, J. B. Kobler, S. M. Zeitels and R. Langer, *Biomacromolecules*, 2006, **7**, 3336-3344.
166. Z. Shen, J. Bi, B. Shi, D. Nguyen, C. J. Xian, H. Zhang and S. Dai, *Soft Matter*, 2012, **8**, 7250-7257.
167. H. Fernandes, K. Dechering, E. Van Someren, I. Steeghs, M. Apotheker, A. Leusink, R. Bank, K. Janeczek, C. Van Blitterswijk and J. de Boer, *Tissue Engineering Part A*, 2009, **15**, 3857-3867.
168. A. Takahashi, T. Kato and M. Nagasawa, *The Journal of Physical Chemistry*, 1967, **71**, 2001-2010.
169. M. Nagasawa and Y. Eguchi, *The Journal of Physical Chemistry*, 1967, **71**, 880-888.
170. H. Sudo, H. A. Kodama, Y. Amagai, S. Yamamoto and S. Kasai, *J. Cell Biol.*, 1983, **96**, 191-198.
171. Y. K. Lee, J. Song, S. B. Lee, K. M. Kim, S. H. Choi, C. K. Kim, R. Z. LeGeros and K. N. Kim, *Journal of Biomedical Materials Research Part A*, 2004, **69A**, 188-195.
172. K. Isama and T. Tsuchiya, *Biomaterials*, 2003, **24**, 3303-3309.
173. C. B. Khatiwala, S. R. Peyton and A. J. Putnam, *American Journal of Physiology-Cell Physiology*, 2006, **290**, C1640-C1650.
174. L. D. Quarles, D. A. Yohay, L. W. Lever, R. Caton and R. J. Wenstrup, *J. Bone Miner. Res.*, 1992, **7**, 683-692.
175. D. Wang, K. Christensen, K. Chawla, G. Z. Xiao, P. H. Krebsbach and R. T. Franceschi, *Journal of Bone and Mineral Research*, 1999, **14**, 893-903.
176. R. T. Franceschi, B. S. Iyer and Y. Cui, *Journal of Bone and Mineral Research*,, 1994, **9**, 843-854.
177. C. Wang, R. R. Varshney and D.-A. Wang, *Advanced drug delivery reviews*, 2010, **62**, 699-710.
178. J. Sun, W. Q. Xiao, Y. J. Tang, K. F. Li and H. S. Fan, *Soft Matter*, 2012, **8**, 2398-2404.
179. R. M. Salasznyk, W. A. Williams, A. Boskey, A. Batorsky and G. E. Plopper, *Journal of Biomedicine and Biotechnology*, 2004, 24-34.
180. S. R. Chastain, A. K. Kundu, S. Dhar, J. W. Calvert and A. J. Putnam, *Journal of Biomedical Materials Research Part A*, 2006, **78A**, 73-85.
181. C. N. Salinas and K. S. Anseth, *Biomaterials*, 2008, **29**, 2370-2377.
182. C. N. Salinas, B. B. Cole, A. M. Kasko and K. S. Anseth, *Tissue Engineering*, 2007, **13**, 1025-1034.
183. X. Jia, J. A. Burdick, J. Kobler, R. J. Clifton, J. J. Rosowski, S. M. Zeitels and R. Langer, *Macromolecules*, 2004, **37**, 3239-3248.
184. H. P. Tan, C. R. Chu, K. A. Payne and K. G. Marra, *Biomaterials*, 2009, **30**, 2499-2506.
185. A. T. Hillel, S. Unterman, Z. Nahas, B. Reid, J. M. Coburn, J. Axelman, J. J. Chae, Q. Guo, R. Trow and A. Thomas, *Science Translational Medicine*, **3**, 93ra67-93ra67.
186. T. Tominaga, V. R. Tirumala, S. Lee, E. K. Lin, J. P. Gong and W.-l. Wu, *The Journal of Physical Chemistry B*, 2008, **112**, 3903-3909.
187. S.-Y. Fu, X.-Q. Feng, B. Lauke and Y.-W. Mai, *Composites Part B: Engineering*, 2008, **39**, 933-961.
188. T. Kauly, B. Keren, A. Siegmann and M. Narkis, *Polymer composites*, 1996, **17**, 806-815.
189. C. Verbeek, *Materials Letters*, 2003, **57**, 1919-1924.
190. M. Lutolf, J. Lauer-Fields, H. Schmoekel, A. Metters, F. Weber, G. Fields and J. Hubbell, *Proceedings of the National Academy of Sciences*, 2003, **100**, 5413-5418.
191. M. P. Lutolf, *Integrative Biology*, 2009, **1**, 235-241.
192. Y. Gong, K. Su, T. T. Lau, R. Zhou and D.-A. Wang, *Tissue Engineering Part A*, 2010, **16**, 3611-3622.
193. Y. Tsuda, M. Yamato, A. Kikuchi, M. Watanabe, G. Chen, Y. Takahashi and T. Okano, *Advanced Materials*, 2007, **19**, 3633-3636.
194. M. Shin, K. Matsuda, O. Ishii, H. Terai, M. Kaazempur-Mofrad, J. Borenstein, M. Detmar and J. P. Vacanti, *Biomedical Microdevices*, 2004, **6**, 269-278.
195. C. Fidkowski, M. R. Kaazempur-Mofrad, J. Borenstein, J. P. Vacanti, R. Langer and Y. Wang, *Tissue Engineering*, 2005, **11**, 302-309.
196. M. Tanihara, Y. Suzuki, E. Yamamoto, A. Noguchi and Y. Mizushima, *Journal of biomedical materials research*, 2001, **56**, 216-221.

197. J.-Y. Lee, S.-H. Nam, S.-Y. Im, Y.-J. Park, Y.-M. Lee, Y.-J. Seol, C.-P. Chung and S.-J. Lee, *Journal of Controlled Release*, 2002, **78**, 187-197.
198. J. Pieper, T. Hafmans, P. Van Wachem, M. Van Luyn, L. Brouwer, J. Veerkamp and T. Van Kuppevelt, *Journal of biomedical materials research*, 2002, **62**, 185-194.
199. J. Rouwkema, J. D. Boer and C. A. V. Blitterswijk, *Tissue Engineering*, 2006, **12**, 2685-2693.
200. S. Fuchs, A. Hofmann and C. J. Kirkpatrick, *Tissue Engineering*, 2007, **13**, 2577-2588.
201. R. E. Unger, A. Sartoris, K. Peters, A. Motta, C. Migliaresi, M. Kunkel, U. Bulnheim, J. Rychly and C. James Kirkpatrick, *Biomaterials*, 2007, **28**, 3965-3976.